



HAL
open science

Description and evaluation of a surface runoff susceptibility mapping method

L.R. Lagadec, Pierre Patrice, Isabelle Braud, B. Chazelle, L. Moulin, J.
Dehotin, E. Hauchard, Pascal Breil

► **To cite this version:**

L.R. Lagadec, Pierre Patrice, Isabelle Braud, B. Chazelle, L. Moulin, et al.. Description and evaluation of a surface runoff susceptibility mapping method. *Journal of Hydrology*, 2016, 541 (PART A), pp.495-509. 10.1016/j.jhydrol.2016.05.049 . hal-02605193

HAL Id: hal-02605193

<https://hal.inrae.fr/hal-02605193v1>

Submitted on 16 May 2020

HAL is a multi-disciplinary open access archive for the deposit and dissemination of scientific research documents, whether they are published or not. The documents may come from teaching and research institutions in France or abroad, or from public or private research centers.

L'archive ouverte pluridisciplinaire **HAL**, est destinée au dépôt et à la diffusion de documents scientifiques de niveau recherche, publiés ou non, émanant des établissements d'enseignement et de recherche français ou étrangers, des laboratoires publics ou privés.

1 **Special Issue of Journal of Hydrology:**

2 SI: Flash Floods and Landslides

3
4 **Title:**

5 Description and evaluation of a surface runoff susceptibility mapping method

6
7 **Authors:**

8 Lilly-Rose Lagadec^{1,2,*}, Pierre Patrice², Isabelle Braud², Blandine Chazelle.¹, Loïc Moulin¹, Judicaël
9 Dehotin¹, Emmanuel Hauchard³, Pascal Breil²

10 **Affiliations:**

11 ¹ SNCF Réseau, Engineering and Project Direction, 6 avenue François Mitterrand, 93574, La Plaine
12 Saint Denis, France.

13 ² IRSTEA, HHLY, Hydrology-Hydraulic Department, Centre de Lyon-Villeurbanne, 5 rue de la Doua,
14 69626 Villeurbanne, France.

15 ³ Agglomeration community of Le Havre (CODAH), 19 rue Georges Braque 76085 Le Havre Cedex,
16 France / UMR M2C 6143 CNRS Geology Department University of Rouen, France

17 Correspondence to: Lilly-Rose Lagadec (lr Lagadec@gmail.com)

18
19 **Keywords:** surface runoff; soil erosion; GIS mapping; evaluation; susceptibility map; transportation
20 network

Abstract

21 Surface runoff is the hydrological process at the origin of phenomena such as soil erosion, floods out
22 of rivers, mudflows, debris flows and can generate major damage. This paper presents a method to
23 create maps of surface runoff susceptibility. The method, called IRIP (Indicator of Intense Pluvial
24 Runoff, French acronym), uses a combination of landscape factors to create three maps representing
25 the susceptibility (1) to generate, (2) to transfer, and (3) to accumulate surface runoff. The method
26 input data are the topography, the land use and the soil type. The method aims to be simple to
27 implement and robust for any type of study area, with no requirement for calibration or specific
28 input format. In a second part, the paper focuses on the evaluation of the surface runoff
29 susceptibility maps. The method is applied in the Lézarde catchment (210 km², northern France) and
30 the susceptibility maps are evaluated by comparison with two risk regulatory zonings of surface
31 runoff and soil erosion, and two databases of surface runoff impacts on roads and railways.
32 Comparison tests are performed using a standard verification method for dichotomous forecasting
33 along with five verification indicators: accuracy, bias, success ratio, probability of detection, and false
34 alarm ratio. The evaluation shows that the susceptibility map of surface runoff accumulation is able
35 to identify the concentrated surface runoff flows and that the susceptibility map of transfer is able to
36 identify areas that are susceptible to soil erosion. Concerning the ability of the IRIP method to detect
37 sections of the transportation network susceptible to be impacted by surface runoff, the evaluation
38 tests show promising probabilities of detection (73 to 90%) but also high false alarm ratios (77 to
39 92%). However, a qualitative analysis of the local configuration of the infrastructure shows that
40 taking into account the transportation network vulnerability can explain numerous false alarms. This
41 paper shows that the IRIP method can be a valuable tool to facilitate field analysis and perform
42 surface runoff zonings and opens interesting prospects for the use of the IRIP method in a context of
43 risk management.

44 1. Introduction

45 Intense surface water runoff is a hydrological process which can generate major damage. When the
46 surface water concentrates, it gains enough energy to erode soil particles, which makes the water
47 denser and more powerful (Wischmeier, 1959). Intense surface runoff includes phenomena such as
48 soil erosion, floods out of river networks, mudflows, and debris flows. According to the Gaspar
49 French database¹, which collects information on natural disasters at a district level, around 40% of
50 flood damage is due to intense surface runoff in France (Dehotin and Breil, 2011a). Surface runoff
51 often impacts populations and infrastructures such as homes or transportation networks (Chazelle et
52 al., 2014). The environment can also be impacted by surface runoff through soil loss and the transfer
53 of pollutants contained in soils.

54 For this study, surface runoff is defined as water from precipitation which does not infiltrate into the
55 soil and flows on the surface until it reaches a permanent river. This hydrological process can also be
56 called overland flow (Hewlett, 1982). Two surface-runoff generation processes can be distinguished:
57 infiltration excess overland flow, when the rain intensity is higher than the soil infiltration capacity,
58 called hortonian runoff (Horton, 1933); and saturation overland flow, when soil storage capacity is
59 limited or the soil is already saturated (Hewlett and Hibbert, 1967). These processes are difficult to
60 observe in the field because they occur quickly and they can occur simultaneously (Cros-Cayot,
61 1996). In general terms, surface runoff is a difficult-to-measure phenomenon (Dehotin et al., 2015).
62 Once surface water flows downstream, it can infiltrate, be transferred or be accumulated –
63 depending on topographical and micro-topographical features – or join a watercourse or drainage
64 system. Surface runoff can flow in a diffuse or concentrated manner. Many factors can influence or
65 reduce surface runoff in a catchment: soil characteristics (type, thickness, roughness, permeability)
66 (Piney, 2009), initial water content, land use (vegetation, urbanization, agricultural land), geology
67 (Onda et al., 2001), topography, geomorphology (ability to concentrate, plateau/valleys distribution)
68 (Douvinet et al., 2008), and rainfall characteristics (intensity, frequency, duration) (Galevski, 1955).

69 In the field of risk management, some terms can have a wide range of definitions, depending on the
70 field of application (Christensen et al., 2003; Thywissen, 2006). The following definitions are retained.
71 Firstly, intense surface runoff is a natural hazard, which means a natural event, potentially
72 dangerous, occurring randomly in space and time (UNDRO, 1979). Risks induced by intense surface
73 runoff are impacts that surface runoff may potentially cause to society (people, goods, environment,
74 economy, etc.). A risk is the combination of a hazard and a vulnerability (UNDHA, 1992). Vulnerability

¹ <https://www.data.gouv.fr/fr/datasets/gaspar/>

75 is often defined as a measure to assess the quantity of loss potentially generated by a hazard (Buckle
76 et al., 2000; Society for Risk Analysis, 2015). In this study, the vulnerability of the transportation
77 network refers to its structural vulnerability; the higher the vulnerability, the higher the possibility of
78 being physically damaged.

79 In the scientific literature, there are many models for the simulation or mapping of surface runoff
80 processes. They may be classified into various approaches: naturalistic, topographic, a combination
81 of criteria or hydrological modeling. Naturalistic approaches often provide results consistent with the
82 reality but they require a very good understanding of the study area, can be applied to rather small
83 areas, and are difficult to replicate (Abudi et al., 2012; Dehotin et al., 2015a; Holzmann and Sereinig,
84 1997; Tetzlaff et al., 2007). Topographical approaches using information from Digital Elevation
85 Models (Delahaye et al., 2002; Langlois and Delahaye, 2002; Pons et al., 2010) have the advantage of
86 being simple and can be automated but the mapping of surface runoff needs to take into account
87 many other parameters such as land use or soil type. Criteria combination approaches also remain
88 relatively straightforward while taking into account multiple parameters. The review of existing
89 methods reveals that most of them focus on water erosion or landslide (Akgun and Türk, 2010;
90 Faulkner et al., 2010; Guillobez et al., 2000; Le Bissonnais et al., 2002; Schmocker-Fackel et al., 2007).
91 Hydrological modeling techniques are both accurate and provide quantitative results including the
92 time evolution of the processes (Carpenter et al., 1999; Cerdan et al., 2002; Dabney et al., 2011;
93 DeRoo et al., 1996; Laflen et al., 1991; Smith et al., 1995). Some are extremely complex. They require
94 significant computational time, calibration to be applied to different catchments, and a large quantity
95 of data. This rapid overview shows that there are multiple methods for surface runoff mapping but
96 the maps are either difficult to reproduce automatically, need many complex input data, or the
97 method is focused on a specific phase of the phenomenon (the accumulation areas, the low
98 infiltration areas or the erosion areas) and do not address all the aspects of the entire runoff process.
99 For this reason, a method called IRIP for Indicator of Intense Pluvial Runoff (French acronym) has
100 been developed to produce comprehensive mapping of areas susceptible to generate, to transfer,
101 and to accumulate surface runoff without explicit hydrological modeling and using open access data
102 (Dehotin et al., 2015a; Dehotin and Breil, 2011a). This automatic method can be applied to a large
103 range of study area sizes with data at various resolutions. However, the validity and relevance of the
104 produced maps must be evaluated carefully and rigorously.

105 The evaluation of hazard models is an important step in model developments. Indeed, model outputs
106 can be used for stakeholder decision-making in risk management. The stakes are very high (cost of
107 structural and organizational adjustments, safety risks) and wrong decisions can lead to serious
108 consequences. It is essential to know the exact value of model outputs, that is, the assumptions

109 made, the application range, and uncertainties related to the results. Globally, model evaluation
110 suffers from a lack of methodological guidelines (Moriassi et al., 2007). For surface runoff hazard
111 models, the evaluation is particularly complex because of the lack of surface runoff data. The
112 phenomenon rapidity and scarcity make large-scale observation and instrumentation a complex issue
113 (Dehotin et al., 2015a; Hudson, 1993). The IRIP method has already undergone numerous evaluations
114 using in-situ measurements (Dehotin et al., 2015a; Laverne, 2013) and discharge data (Arnaud and
115 Dehotin, 2011; Legros, 2014) but to go further in the evaluation procedure and to assess the
116 relevance of the IRIP method from the point of view of risk assessment, the use of proxy data is
117 suggested. Proxy data are data which are not direct measurements of the phenomenon but are
118 related to it and provide large-scale evidence of the phenomenon occurrence (IPCC, 2003). Some
119 studies in hydrology use proxy data to evaluate models, such as flooded road reports (Naulin et al.,
120 2013; Versini et al., 2010a, 2010b), observations of gravitational hazards in mountainous areas
121 (Defrance, 2014), and post-event surveys (Javelle et al., 2014; Ortega et al., 2009). Concerning the
122 IRIP method evaluation, few comparisons have been performed with proxy data such as surface
123 runoff impact locations on railways (Dehotin et al., 2015b) and natural disaster declaration locations
124 from the Gaspar French database (Dehotin and Breil, 2011a). However, these tests have been
125 performed for few case studies and remain qualitative. Indeed, the comparison between model
126 outputs and proxy data generates technical issues: for example, how can data that are different in
127 form and content and that do not carry the same information be compared reliably? The use of proxy
128 data highlights the lack of methodological framework but also shows the valuable contribution of this
129 type of data for model evaluation.

130 The first objective of this paper is to present the IRIP method for surface runoff susceptibility
131 mapping. The second objective is to evaluate the IRIP maps by comparison with different types of
132 proxy data available on the study area: regulatory zonings of surface runoff and soil erosion and
133 databases of surface runoff impacts on roads and railways. The paper proposes an evaluation
134 method that allows quantitative evaluation of the spatial information contained in the IRIP maps.
135 Finally, development paths are discussed to adapt the IRIP method as a tool for risk management.

136 **2. Materials and Methods**

137 **2.1. The IRIP Method**

138 IRIP is a method to map the spatial distribution of areas susceptible to surface runoff. The IRIP
139 method concept is based on the creation of three susceptibility maps which represent surface runoff
140 generation, transfer, and accumulation. Note that, to obtain a hazard map, the rainfall must be taken
141 into account and to get a risk map, the hazard map must be combined with the stakes of the study

142 area and their vulnerabilities. These two aspects are not considered in the present study, which only
143 focuses on the susceptibility maps provided by the IRIP method.

144 Each susceptibility map (generation, transfer, and accumulation) is created by combining five
145 indicators, summarised in Table 1 (columns 1&2). Each indicator is classified in two categories
146 favourable (1) or not favourable (0) to surface runoff (Table 1, col 3), providing a binary map. The five
147 maps are subsequently assembled to produce a surface runoff susceptibility map from 0 (not
148 susceptible) to 5 (very susceptible). This method is applied for the three IRIP maps, as represented in
149 Figure 1. After reclassification, the generation map becomes an input indicator for the two other
150 maps of transfer and accumulation. The reclassification proceeds as follows: a pixel is favourable
151 (score = 1) if the generation susceptibility levels in its relative drained area have a mode (the most
152 present value of the distribution) higher than a user-defined susceptibility level (3 by default). The
153 use of the generation map as an input for the two others means that susceptibility to transfer or
154 accumulation is conditioned by a sufficiently high susceptibility for surface runoff generation. This
155 allows the incorporation of an upstream-downstream logic in the maps. For each map, the five
156 indicators have been chosen based on field knowledge (Dehotin et al., 2015a), literature review
157 (Dehotin and Breil, 2011b), and multiple combination tests.

158 For the surface runoff generation map, the five indicators are derived from factors influencing runoff
159 generation: soil properties, topography, and land use. Three indicators represent the impact of soil
160 properties and are based on soil erosion model parameters (Le Bissonnais et al., 2002; Le Gouee et
161 al., 2010; Nearing et al., 1989). The erodibility indicator in the generation map represents the
162 possibility of the generated surface water combining with soil particles to generate a mudslide
163 (Cerdà and Doerr, 2008). For agricultural plots, the erodibility indicator also represents the
164 susceptibility of soils to create slaking crusts that are favourable to surface runoff generation. The
165 topography indicator is an “or” combination of the slope and the topographic index, that is, the
166 topography indicator is favourable if the slope is steep, if the topographic index is high, or both.
167 Steep slopes are considered as favourable to surface runoff generation reflecting the reduced ability
168 of water to infiltrate into the soil. The topographic index (Beven and Kirkby, 1979), $\ln(a/\tan b)$, where
169 a is the upstream drained area and b is the local slope, reflects the capacity at one point to evacuate
170 water from upstream, that is, water storage-prone areas. Although the topographic index also uses
171 the slope, the topography indicator in the IRIP method combines two different effects: slope and
172 ability to store water. In order to be able to apply the method in every catchment without local
173 knowledge, relative thresholds (t_1 , t_2) are used to distinguish topographic indicators (slopes,
174 topographic index) as favourable or not. For each indicator, the distinction is made thanks to
175 classification algorithms (MacQueen, 1967; Reuter et al., 2006). It permits dividing the study area

176 into two categories of slopes or topographic indices depending on the local and surrounding pixel
177 values. The land use indicator reflects the fact that urban and agricultural areas are considered as
178 favorable to surface runoff generation. For urban areas, the generation map is recalculated to force
179 soil permeability and thickness to be favourable in those areas, in the event that the areas have not
180 been classified as favourable from the indicators derived from the soil map.

181 The susceptibility maps of surface runoff transfer and accumulation reflect surface water natural-
182 flow dynamics. Both involve different mechanisms, acting often in the opposite direction, such as
183 slope and break of slope. This is why two maps are created. The choice of the corresponding
184 indicators is based on detailed analyses of past intense surface runoff events (Dehotin and Breil,
185 2011b) where slope, break of slope, catchment compactness, and artificial linear axes appeared as
186 main factors to produce intense phenomena. The computation of the break of slope proceeds as
187 follows: in each pixel, the mode of the slope value distribution in the upstream area drained by this
188 pixel is computed and compared to the local slope value of the pixel. If the upstream slope mode is
189 smaller (respectively higher) than the local slope, the pixel is indicated as convex (respectively
190 concave), and is assigned 1 for the transfer map (1 for the accumulation map). The transfer map uses
191 the Horton form factor (Horton, 1932), which is the ratio of area to length of the sub-watershed
192 defined by the drained area at the considered pixel. The artificial linear axes are taken into account in
193 the transfer map because of their role in surface runoff interception and displacement (Cerdà, 2007;
194 Pams-Capoccioni et al., 2015).

195 Finally, the input data of the IRIP method are: a DEM, a land use map, a soil map, and optionally the
196 artificial drainage network (Figure 1). The input data resolution can be adapted to the size of the
197 study area. For a relatively large study area, the analyst can proceed as follows: maps can be initially
198 produced for the whole study area with a coarse resolution DEM (i.e. cells larger than 10 meters) and
199 then areas susceptible to surface runoff can be focussed on with a higher resolution DEM (i.e. cells
200 smaller than 10 meters). These susceptibility maps reflect a certain description of the surface runoff
201 mechanisms in a watershed. Given the considered indicators, the IRIP map of surface runoff
202 generation highlights the areas more susceptible to generate water on the soil surface. The IRIP
203 transfer map highlights the areas where surface water can move and gain speed, and the IRIP map of
204 accumulation highlights the areas where there is a tendency for a reduction in surface water velocity
205 and water level increases. The method aims to be simple to implement, using open-access input data
206 and to be robust regardless of the data quality and uncertainty. This is the reason why more complex
207 methods such as weighting the indicators or classifying them into more than two categories were not
208 retained in the first version of the method. However, the method remains open for adaptation
209 regarding the user knowledge, but the default parametrization permits applying the method

210 whatever the study area. In this paper, the relevance of the IRIP maps is assessed based on this first
211 version of the method.

212 **2.2. The Study Area**

213 The Lézarde catchment (210 km²), located between the English Channel and the Seine river, is well-
214 known for being subject to flooding predominantly generated by surface runoff (Delahaye et al.,
215 2002; Douvinet et al., 2014; Le Gouee et al., 2010). The catchment morphology is composed of large
216 plateaux and narrow valleys (Figure 2). The permanent hydrographic network is very short but the
217 temporary network consists of an extremely dense talweg network. The area was formed during the
218 last glacial era during which the ice melt eroded the soil surface (Auzet et al., 1993). Soil
219 characteristics of the catchment are mostly silt and clay with flint stones. Locally, there are sandy
220 loams that increase soil erosion processes. The geology of the territory is composed of karst which
221 forms a complex active underground river network (Hauchard and Laignel, 2008). The climate of the
222 whole Seine-Maritime region is characterised by two main rainfall seasons: summer and autumn. In
223 summer, rainfall durations are shorter than in autumn but more intense, whereas in autumn the
224 rainfall patterns are less intense but last for long periods, leading to soil saturation (Douvinet, 2008).
225 These two rainfall patterns can both generate storm runoff floods but involve different mechanisms.
226 In terms of land use, a large part of the Lézarde catchment is made up of agricultural areas. A soil
227 crusting process takes place between planting cycles, influenced by an exposed and high silt rate in
228 the top soil, making the soil surface almost impervious (Robinson and Phillips, 2001). In addition,
229 roads and villages were built in exposed areas: many roads are located in talwegs and villages are
230 located at the downstream end of catchments or sub-catchments. Consequently, flooding in the
231 catchment tends to generate major damage.

232 In the Lézarde catchment, the IRIP maps were produced using a 25-meter DEM from the French
233 National Institute of Geograh². The land use map³ is on the scale of 1/5000 in rural areas and 1/2000
234 in urban areas. The soil map is the pedologic map from the French National Institute for Agronomic
235 Research (INRA) at the scale of 1/1000000 (Dupuis, 1969). To calibrate the method in the Lézarde
236 catchment, some assumptions are made based on literature review, discussions with local
237 stakeholders and multiple tests on the IRIP maps. For the soil indicators, the distinction between
238 favorable or not is based on soil data analysis (Daroussin and King, 1997; Jamagne et al., 1995). The
239 slope threshold for the distinction between favorable or not was fixed at 4%, based on surface runoff
240 studies on the Lézarde catchment (Hauchard, 2002). For the land use indicator, the urbanized and

² <http://professionnels.ign.fr/bdalti>

³ <http://mos.hautenormandie.fr/Presentation>

241 the agricultural areas are considered as favorable to surface runoff (Hauchard et al., 2002). For the
242 Horton form factor, the index is considered as favorable to surface runoff transfer for values larger
243 than 0.15 (fixed from tests with IRIP maps). Only roads and railways are used for the artificial linear
244 axes, as data on agricultural drainage are not available at this scale. The flow accumulation threshold
245 was chosen at 0.5 ha, a value small enough to detect surface runoff close to the catchment head.
246 These choices are explained further in the discussion and perspectives section.

247 **2.3. The Comparison Data**

248 The data sets used for the evaluation of the surface runoff susceptibility maps are presented here.
249 Four data sets are used: two regulatory zonings of surface runoff and erosion risks and two data sets
250 of surface runoff impacts on roads and railways networks. The two regulatory zonings are provided
251 by the agglomeration of Le Havre⁴ and the local association of the Pointe de Caux Catchment⁵
252 (SMBV) respectively. They are part of the natural risk prevention plan (Departmental Directorate of
253 Seine-Maritime, 2013a; Departmental Directorate of Seine-Maritime, 2013b). These regulatory
254 zonings take into account both exposure of assets at risk and their probability of damage. The
255 database of surface runoff impacts on roads is provided by the SMBV and the database of surface
256 runoff impacts on railways is provided by the French National Railway Company (SNCF Réseau).

257 **2.3.1. The Surface Runoff Regulatory Zoning**

258 The surface runoff zoning was established in a qualitative manner. All the surface runoff axes, where
259 water can concentrate (i.e. the dry talwegs), were identified by field expertise and historical
260 information on past events (Hauchard, 2002). Then, to create the surface runoff zoning, a buffer area
261 around surface runoff axes was designed. The buffer size ranges from 5 to 80 meters and the value
262 was locally chosen thanks to field knowledge. Finally, hydrological modeling was used only in areas
263 with high exposure levels to obtain water levels and flow velocities, but the latter information is not
264 used in the evaluation procedure, where only the zoning map is used. This zoning map does not take
265 into account the presence of protection structures against floods.

266 For the comparison with IRIP, the surface runoff zoning is compared with the IRIP map of surface
267 runoff accumulation susceptibility. The zoning is created from the dry talweg axes, which are axes of
268 water concentration and where, locally, water velocity reduces and subsequently water depth
269 increases. This effect is included in the IRIP map of accumulation and is represented by the IRIP
270 indicators: flow accumulation, topographic index, and concave break of slopes. For the comparison

⁴ <http://www.codah.fr/article/lutte-contre-les-inondations>

⁵ http://www.smbv-pointedecaux.fr/web/decret_erosion2.html

271 tests, the permanent hydrographic network is also masked. Indeed, the accumulation map also
272 detects the rivers but the comparison rather focuses on hillslopes where surface runoff occurs.

273 **2.3.2. The Soil Erosion Regulatory Zoning**

274 The soil erosion zoning was created using two soil erosion models: the RUSLE model from USDA
275 (Dabney et al., 2011) and the STREAM model from INRA (Cerdan et al., 2002). The models have been
276 adjusted using erosion traces from aerial photographs. The results of the two models have been
277 combined and validated by knowledge from local experts. The soil erosion hazard map was crossed
278 with a map of the territory vulnerabilities to obtain the soil erosion zoning map.

279 For the comparison with IRIP, the soil erosion zoning is compared with the IRIP map of surface runoff
280 transfer susceptibility. Indeed, the soil erosion is a process influenced by the occurrence of surface
281 runoff with a water level and a speed sufficient to transport materials. This effect is included in the
282 IRIP map of transfer and is represented by the IRIP indicators: compactness index and convex break
283 of slopes. For the comparison tests, the urban areas are masked because the regulatory zoning
284 focuses on rural areas.

285 **2.3.3. The Databases of Impacts on Transportation Networks**

286 The database of flooded roads is made up of 31 road sections and was created after an intense
287 rainfall event by witness interviews and field expertise. On October 13, 2013, the Lézarde catchment
288 was subject to a significant rainfall event, generating intense surface runoff. The return period of the
289 event was estimated to be more than a hundred years by the Predict weather services (Gouvazé and
290 SMBV, 2013). The high-intensity rainfall affected mainly the three sub-catchments located in the
291 north of the Lézarde catchment, upstream of the Lézarde River (highlighted in yellow in Figure 3). Up
292 to 70 mm fell in 6 hours in this area and the three rain gages (1, 2, 3) recorded 160, 156 and 100 mm
293 respectively in 24 hours. Thus the comparison tests focus only on these 3 sub-catchments. The road
294 sections in the database were temporarily cut off by floodwater and impracticable or even swept
295 away by floodwater (photos at the bottom of Figure 3).

296 The database of impacts on the railway is made up of 41 incidents listed from 1995 to 2012. These 41
297 incidents are observed in 21 railway sections, the incidents occurring sometimes at the same
298 location. This database is not exhaustive and contains uncertainties on incident locations, particularly
299 in relation to the source of flooding and the length of railway that was affected. The recorded types
300 of incidents are embankment erosion, flooded platforms or mudslides. For the comparison tests,
301 these two databases are compared to the IRIP maps of transfer and accumulation susceptibility,
302 because we assume that accumulation as well as transfer of water can generate damage.

303 This section highlights that the four data sets differ greatly in form and content. The next section
304 describes the methodology used to compare these four data sets to the IRIP surface runoff
305 susceptibility maps.

306 **2.4. The Evaluation Method**

307 To evaluate the IRIP method, the surface runoff susceptibility maps are compared to a set of
308 comparison data. In this section, the comparison tests and the verification indicators are presented,
309 as well as the data formatting process that is required to compare different data types.

310 2.4.1. Comparison Tests

311 To assess the correspondence between the IRIP maps and the comparison data, contingency tables
312 are created and associated verification indicators are computed. This method is inspired by the
313 standard verification methods for dichotomous (yes/no) forecasts (Hogan and Mason, 2012; Stanski
314 et al., 1989). Table 2 shows the theoretical contingency table created for each comparison test. The
315 “observed event” columns represent information from the comparison data. For example, in the case
316 of the zonings, “yes” means inside the zoning and “no” means outside. In the case of the impact
317 databases, “yes” means the impacted network section and “no” means the remaining parts of the
318 transportation network that were not impacted. The “IRIP” lines represent information from the IRIP
319 maps. For the tests, the IRIP maps are converted into dichotomous results, with “yes” being pixels
320 with a susceptibility level greater than or equal to 4 and “no” being pixels lower than 4. The
321 threshold of 4 is chosen regarding the low proportion of susceptibility level values of 4 and 5 over the
322 catchment. Pixel values of 4 and 5 represent 4% of the study area in average, whereas pixel values of
323 3 represents 30% of the study area. In the theoretical contingency table, for comparisons with the
324 regulatory zonings (respectively, comparisons with the impacts on the transportation network), true
325 positives are IRIP pixels with high susceptibility levels located inside the zonings (resp. inside the
326 impacted network sections). True negatives are IRIP pixels with low susceptibility levels located
327 outside the zonings (resp. inside the not impacted network sections). False positives are IRIP pixels
328 with high susceptibility levels located outside the zonings (resp. inside the not impacted network
329 sections). Finally, false negatives are IRIP pixels with low susceptibility levels located inside the
330 zonings (resp. inside the impacted network sections). From the contingency tables, five verification
331 indicators are computed: accuracy, bias, success ratio (SR), probability of detection (POD), and false
332 alarm ratio (FAR). POD and FAR are computed only when comparing with the impacts on the
333 transportation network, in order to assess the ability of the IRIP method to detect areas susceptible
334 to be impacted. The indicators are presented in Table 3 along with the formulas and the result
335 interpretations.

336 2.4.2. Data Formatting

337 Concerning comparison tests with the regulatory zonings, the surface runoff regulatory zoning is
338 compared with the IRIP map of accumulation susceptibility. The soil erosion zoning is compared with
339 the IRIP map of transfer susceptibility. For each comparison, the contingency table is computed by
340 using two different thresholds of IRIP susceptibility level: for pixel values greater than or equal to 4
341 and for pixel values of 5 only. Moreover, for each comparison, the contingency table is computed by
342 using three different sizes of buffer area around the zonings: 0, 25, and 50 meters. Buffer areas are
343 used in order to compensate for uncertainties in data comparison. Uncertainties can come from the
344 fact that different data formats are compared (raster for the IRIP map and polygons for the zonings).
345 This can lead to uncertainty when overlapping the data. Uncertainties can also come from the input
346 data used for the creation of the IRIP maps and the zonings (i.e. DEM resolution). Buffer area sizes of
347 0, 25, and 50 meters correspond to a shift of zero, one or two pixels of the IRIP maps.

348 Concerning the impact databases, comparison tests are performed separately for roads and railways,
349 and for each test, the impact locations are compared with the IRIP maps of transfer and
350 accumulation simultaneously. The comparisons are performed using the transportation network as
351 the reference study area, and not the whole catchment. In order to perform the comparison, the
352 linear transportation networks are transformed to polygons, using a buffer. Two buffer area sizes of
353 25 and 50 meters on both sides of the transportation network were considered. Concerning the IRIP
354 maps, an area is considered susceptible to surface runoff if there is a spatial persistence of pixels
355 with high susceptibility levels, and not if there is only one isolated pixel with a high value. The pixel
356 spatial persistence on the IRIP maps of transfer and accumulation is taken into account as follows: a
357 buffer area of 25 meters is drawn around all pixels of values 4 and 5 and, if an isolated pixel with its
358 buffer area is not intercepted by another buffer, the pixel is removed (Figure 4a). Finally, four
359 contingency tables are computed for roads and railways with two different buffer area sizes around
360 the transportation network, focusing on the overlapping surface between the IRIP maps and the
361 impacted road sections, as presented in Figure 4b.

362

363 3. Results

364 3.1. Application of the IRIP method in the Lézarde catchment

365 The susceptibility map of surface runoff generation (Figure 5) shows that the catchment presents a
366 high susceptibility to generate surface runoff. About 88% of the study area has pixels with a score
367 above 3, on a scale ranging from 0 to 5. The pixels with a highest score are located in the urban areas

368 of Le Havre and Montivilliers. We can also see high susceptibility levels in the western part of the
369 catchment and in the valley sides. Although the valley sides are occupied by forest, they present a
370 high susceptibility to generate surface runoff because of soil properties and steep slopes. Despite the
371 flat topography of the plateaux upstream of the catchment, they present a high susceptibility to
372 surface runoff generation with values of 3 and 4 locally because of the soil properties and the
373 agricultural land use. Occupying approximately two thirds of the catchment, these plateaux are
374 responsible for the largest part of the generated surface water.

375 The susceptibility map of surface runoff transfer (Figure 6) mainly shows high levels in the valley
376 sides, where slopes are steep and break of slopes are convex. This map shows low susceptibility
377 values of transfer in the plateaux and in the valley bottom. The high susceptibility areas actually
378 highlight the sides of the main talwegs and a great deal of small talwegs even very close to the head
379 of the catchment.

380 The susceptibility map of surface runoff accumulation (Figure 7) shows that plateaux are prone to
381 accumulate surface runoff with values equal or greater than 3 on a large part of the catchment.
382 These susceptibility levels are due to low slopes, concave break of slopes, and a high topographic
383 index in the upstream portions of the catchment. Permanent rivers are identified with the level 5,
384 and an extremely dense talweg network can be distinguished with the susceptibility levels 4 and 5. In
385 upstream talwegs, susceptibility levels 4 and 5 are still visible but seem to be more spread out. The
386 map highlights that the valley sides are not favorable to surface runoff accumulation in contrast to
387 the map of transfer.

388 **3.2. Evaluation of the IRIP maps**

389 In this section, the IRIP maps are first compared to the regulatory zonings, in order to assess the
390 ability of the map of accumulation to identify areas prone to concentrated surface runoff (Figure 8)
391 and to assess the ability of the map of transfer to identify areas prone to soil erosion (Figure 9). Then,
392 the IRIP maps are compared to the databases of impacts on the transportation network to assess the
393 ability of the IRIP method to identify road and railway sections susceptible to be impacted by surface
394 runoff (Figure 10).

395 The superimpositions of the IRIP maps and the two regulatory zonings (Figures 8 and 9) show a good
396 visual correlation and a relevance of the spatial distribution of the IRIP susceptibility levels. Table 4
397 presents the results of the comparison between the two regulatory zonings and the IRIP maps. Six
398 comparison tests are performed for the surface runoff zoning and six for the soil erosion zoning: with
399 the three buffer area sizes and considering pixels of value 4 and 5, and 5 only. Three indicators are

400 computed for each test: accuracy, bias, and success ratio. Results show that for that comparison with
401 the surface runoff zoning, the accuracy ranges from 0.68 to 0.86 and, for the comparison with the
402 soil erosion zoning, accuracy ranges from 0.36 to 0.69. Biases for all the tests are lower than 1 and
403 range from 0 to 0.41. The success ratio represents the number of high susceptibility level pixels that
404 are located inside the zoning, regarding the whole study area. It ranges from 0.41 to 0.92. The best
405 success ratio for the accumulation map is 0.92 and is obtained when using a 50-meter buffer around
406 the surface runoff zoning and when considering only pixels with a value of 5. The best success ratio
407 for the transfer map is also 0.92 and obtained with the same conditions. Moreover, a success ratio of
408 0.91 is obtained when considering pixels of value 4 and 5, using a 50-meter buffer. Concerning the
409 comparison with the impacts on the transportation network, Table 5 shows the results of the five
410 verification indicators for the four tests: comparison with the database of impact on roads and with
411 the database of impacts on railways, using two different buffer area sizes for both of 25 and 50
412 meters around the transportation network. For the analysis of impacts on roads, comparison tests
413 show accuracy of about 0.6 and 0.3 for impacts on railways. Biases are greater than 1 and range
414 approximately from 3 to 9. Success ratios are lower than 0.25 for both transportation networks.
415 Probabilities of detection range from 0.7 to 0.9, and figures are similar for the false alarm ratios. The
416 best probability of detection for the impacted road sections is 0.73 using a 25-meter buffer around
417 roads, and the best one for the impacted railway sections is 0.9 using a 50-meter buffer around
418 railways.

419 These results are discussed in the next section in the light of the assumptions made for the
420 comparison tests and in the light of the high false alarm ratios for the comparison tests with the
421 impact databases. Moreover, suggestions are presented to go further in the evaluation method and
422 in the development of the IRIP method.

423

424

425

426 **4. Discussion and Perspectives**

427 **4.1. Result Discussion**

428 **4.1.1. Comparisons with the Regulatory Zonings**

429 The success ratio is the number of pixels with high susceptibility levels located inside the zonings
430 regarding the total number of pixels with high susceptibility levels in the catchment. So, without

431 using a buffer, obtaining success ratios of 0.72 and 0.64 is already promising. Using a buffer area of
432 50 meters around the zonings makes it possible to obtain success ratios above 0.9. This shows that a
433 large number of high susceptibility IRIP pixels are located very close to the regulatory zonings and
434 that uncertainties in the high susceptibility level locations could be interpreted as between 0 and 2
435 pixels. These success ratios are extremely promising considering that the two maps are created using
436 very different techniques and that they do not focus exactly on the same areas. The soil erosion
437 zoning focuses on agricultural areas, and the surface runoff zoning focuses on talweg axes, whereas
438 the IRIP method takes into account the whole catchment. Different results are obtained when
439 considering pixel values of 5 and pixel values of 4 and 5 together. The choice of the susceptibility
440 level depends on the information sought. Few pixels with a value of 5 are present in the catchment.
441 They underestimate the global sensitivity of the catchment (bias close to zero), but they are more
442 likely to indicate the localization of the areas that are highly susceptible to surface runoff. Concerning
443 the IRIP map of accumulation, Figure 8 shows that the pixels are located precisely inside the zoning in
444 the downstream part of the catchment but, in the catchment headwaters, pixels with a value of 4 are
445 spread and are located outside the zoning. This spatial persistence of pixel values of 4 could indicate
446 the beginning of a talweg that is not well defined in the landscape. Further comparison tests and field
447 analysis must be undertaken to confirm this hypothesis.

448 Moreover, Figure 9 shows that a considerable section of areas contained in the erosion zoning is not
449 correlated with the IRIP map of transfer, but seems to fit with the IRIP map of accumulation (Figure
450 11). Indeed, these areas present lower slopes, concave break of slopes, high topographic indices, and
451 high flow accumulations. The soil erosion zoning gives a map of soils prone to erosion but, depending
452 on the areas, erosion mechanisms and impacts can be different. The transfer map could emphasize
453 incision susceptibility and the accumulation map could localize the deposit areas. Field analysis must
454 be undertaken to better assess the ability of the IRIP maps to identify different erosion processes,
455 but knowing the spatial distribution of the dominant processes could permit adapting the erosion
456 prevention techniques in terms of the mechanisms involved.

457 Finally, the comparison with the two regulatory zonings shows that the maps produced with the IRIP
458 method seems to be relevant in identifying areas susceptible to surface runoff. Moreover,
459 susceptibility levels of 5 seem to indicate with a certainty of 90% an area susceptible to concentrative
460 surface runoff (for the IRIP map of accumulation) and an area susceptible to soil erosion (for the IRIP
461 map of transfer) with a spatial accuracy from 0 to 2 pixels.

462

463

464 **4.1.2. Comparisons with Impacts on the Transportation Network**

465

466 The probability of detection is the ratio of good detection over the total observed impacts. Obtaining
467 probabilities of detection of 0.7 for road impacts and 0.8 for railway impacts is promising. The IRIP
468 method seems to be relevant in identifying areas susceptible to surface runoff. However, success
469 ratios are low due to a significant number of false alarms (i.e. false positives). The highly significant
470 false alarm ratios and the overestimation are discussed.

471 First, these results come from the fact that the IRIP method gives susceptibility maps regarding soil
472 surface predisposition, but the occurrence of a surface runoff-related impact depends on the rainfall
473 spatial variability. For the rainfall event of October 13, 2013, it is assumed that rainfall was spatially
474 homogeneous in the three sub-catchments, but this hypothesis is no more realistic for the railway
475 network because the study area is wider and the database ranges in time from 1995 to 2012, when
476 rainfall events are not likely to have been homogeneous. This can explain why higher false alarm
477 ratios are obtained for the analysis of railway impacts. Moreover, working with proxy data involves
478 uncertainties. For example, the databases may suffer from a lack of exhaustiveness in the number of
479 reported impacts. In that case, impacts only are reported, whereas some network sections could
480 have been affected by floodwater without being damaged and without network managers being
481 informed. In addition to this, high false alarm ratios can come from the fact that the IRIP maps, which
482 represent a susceptibility of surface runoff occurrence, are compared to an impact which is an
483 effective risk. It is essential to take the structural vulnerability of roads and railways into account for
484 a better assessment of the IRIP maps' ability to identify impacted sections.

485 Concerning the impacted roads analysis, more than 40 hydraulic structures are present over the
486 three sub-catchments where intense rainfall occurred on October 13, 2013. They probably played an
487 important role in the protection of the road network. Figure 10 shows the road network of the three
488 sub-catchments along with the hydraulic structure locations. Post-event investigation allowed
489 reporting whether or not the hydraulic structures have played their protective role. Green points
490 indicate that the structure did not overflow; orange points indicate that it overflowed. This
491 information can already explain why some road sections that appear susceptible to surface runoff
492 with the IRIP method have not been reported as impacted. For example, in Figure 12, the A photo
493 (corresponding to the A area on Figure 10) was taken just after the event and shows that the dam
494 closing a reservoir is at one meter below the overflow. Thus, it could have protected this road section
495 against floodwater. Further discussions with the river basin managers helped to explain some other
496 false alarms. Figure 12 shows photos of three road sections (B, C, and E areas can be seen in Figure

497 10) that are considered as false alarms, despite the absence or dysfunction of protective structures.
498 These photos show the configuration of roads within their environment, and give some clues about
499 the vulnerability level of the sections regarding surface runoff. Photo B shows a large drainage ditch
500 along the road. Photo C shows the road slightly elevated and the low point located in the grassland.
501 These observations have been confirmed by the river basin managers. They also attested that the
502 road section in the A area is regularly flooded by surface runoff during intense rainfall events and
503 that the low point in the D area is not located on the road but in the nearby field. The three impacts
504 in the E area present the same configuration, that is, they transversally cut a dry talweg without any
505 crossing structure. Photo E shows one of these intersections which still have the marks of an intense
506 rainfall event, with standing water and soil deposits gathered in a mound. This configuration can
507 explain why IRIP detects smaller susceptible areas than the reported section for these three impacts.
508 The road may act as a barrier to the water flow path. Water can spread on both sides along the road
509 and consequently flood a large section of the road. Using a DEM with a better resolution could help
510 in identifying the local configuration. Finally, according to the river basin managers, the F area has
511 been less exposed to the rainfall event, which can explain why it has not been reported as impacted.

512 For railways, the infrastructure configuration is more complex. Indeed, railway structures are highly
513 constrained to keep a steady inclination and do not follow the natural topography. Railways are
514 often built on embankments or in cuttings of varying height or depth. These configurations make
515 railways vulnerable to surface runoff. To protect the railway infrastructure, multiple drainage devices
516 or crossing structures are present all along the tracks to intercept flow paths and redirect them
517 downstream. Therefore, to better identify railway sections susceptible to being impacted by surface
518 runoff, the vulnerability must be characterized. The configuration of the infrastructure itself must be
519 defined but the level of maintenance of the hydraulic structures must also be taken into account.

520

521 **4.2. Further Analysis with the Evaluation Method**

522 In the evaluation method, we need to compare data that do not have the same shape, do not give
523 the same information, and that have been acquired using different techniques. Suitable indicators
524 must be used to show the correspondence between data and to quantify it. For example, the success
525 ratio gives information on whether or not the pixels with a high susceptibility level are located inside
526 the zoning, but do not inform on the spatial distribution of the pixels regarding the zoning. For
527 further evaluation, more complex indices could be used in order to improve the correlation analysis,
528 for example by focusing on the shape of strong pixel areas or by analyzing pixel surroundings and
529 mitigating isolated pixel effects (Hagen-Zanker, 2009; Hargrove et al., 2006).

530 For the comparison tests, assumptions have been made and preliminary treatments have been
531 carried out on the comparison data and on the IRIP map. Choices have been made for this study and
532 must be discussed. First, pixels with a value of 4 and 5 are considered as high susceptibility levels.
533 The significance of the susceptibility level 5 has been shown, but the significance of level 4 must be
534 assessed. The significance of level 3 must also be assessed. Is it really not significant? Do levels 0, 1,
535 and 2 indicate no surface runoff sensitivity? Moreover, for the comparison tests, buffer areas have
536 been used. In order to avoid arbitrary choice on the buffer area size, the tests have been performed
537 using 2 different sizes of 25 and 50 meters but more sizes could be tested, particularly negative
538 buffer areas (reducing the zoning). For the comparison with the impacts on the transportation
539 network, the hypothesis on the spatial persistence of high susceptibility levels indicating areas
540 susceptible to be impacted must be assessed, along with the significance of isolated pixels. Do they
541 bring valuable information or noise due to eventual input data inaccuracy?

542 Moreover, this study focuses on the transfer and the accumulation maps. For further evaluation, it
543 would be interesting to focus on the susceptibility map to surface runoff generation and evaluate its
544 ability to detect areas susceptible to generate significant quantities of surface water. For example,
545 for the impact databases, it would be interesting to use the map of generation in a second phase, to
546 help in distinguishing the sections most susceptible to be impacted among the ones detected by the
547 maps of transfer and accumulation. Sections with a large area upstream with high susceptibility
548 levels of surface runoff generation could be susceptible to be impacted with relatively major
549 quantities of water or more often, or to be impacted first during a rainfall event. This hypothesis
550 must be evaluated.

551 For further evaluation of the ability of the IRIP method to detect sections of the transportation
552 network susceptible to be impacted by surface runoff, the structural vulnerability of the network
553 must be characterised. A vulnerability indicator with different levels could be defined on the whole
554 network, in order to combine hazards and vulnerability better and to correlate the location of
555 impacts more effectively. Concerning the impacts, for such a comparison, further research must be
556 undertaken to improve the completeness of the databases. In addition to these tests, particular
557 events must be analyzed in greater detail in order to consider the influence of rainfall characteristics
558 and better assess the surface runoff flow dynamic. To confirm the results obtained in this study,
559 further comparison tests must be performed with different comparison data and for different study
560 areas with other hydrological contexts.

561

562 **4.3. Further Analysis with the IRIP Method Development**

563 Several options for further developing and improving the IRIP method can be proposed. Concerning
564 the map of susceptibility to surface runoff generation, the valley sides appear as favorable to surface
565 runoff whereas in reality the plateaux are the most important sources of surface runoff generation
566 due to their relative importance in terms of proportion of the catchment size and to the fact that
567 they are cultivated. They can generate substantial quantities of surface runoff which can be
568 transferred to the valley throughout the extremely dense dry talweg network. It would be interesting
569 to be able to integrate these geomorphology features in the IRIP method. For example, a
570 computation of geomorphologic indexes could permit calibrating the method in terms of the
571 plateau/valley distribution. The default configuration of the method is that steep slopes are
572 favorable to surface runoff generation, which is relevant for mountainous areas, for example, but
573 this choice could be inversed when working on large flat areas with large agricultural fields.
574 Furthermore, the susceptibility map of surface runoff generation could be improved with better data
575 accuracy. Especially the soil map, which is used for three of the five indicators, has a resolution of
576 1/1000000 and gives only six different soil units in the Lézarde catchment. Moreover, it has been
577 shown that the geology has an influence on surface runoff generation and transfer (Onda et al.,
578 2001); it would be interesting to use this parameter in the IRIP method.

579 The map of susceptibility to surface runoff transfer takes the artificial linear axes as an input indicator
580 because they can modify surface runoff directions, but if the data are available it would be
581 interesting to add the urban and agricultural drainage network in this indicator. For the creation of
582 this map, we currently use the Horton form factor to reflect the compactness effect of the sub-
583 catchment drained by each pixel (0.15 for our study). This index is not particularly satisfying because
584 of its instability when computed on small drained areas. More adapted compactness indexes must be
585 tested (Gravelius, 1914; Schumm, 1956), although their implementation can be complex with GIS
586 techniques (Bardossy and Schmidt, 2002; Bendjoudi and Hubert, 2002). It would be better to use an
587 index that is more adapted to a distributed computation.

588 In addition to these suggestions, the IRIP method could also be improved by making additional tests.
589 For example, stability tests on the indicator thresholds could be performed to evaluate the threshold
590 computation method. Changes in the input data resolution (DEM, land use map, and soil map) could
591 be studied to evaluate how it affects the resulting maps. It would also be interesting, from a risk
592 point of view, to cross the IRIP maps with meteorological data or land use change monitoring to
593 provide real-time probability maps.

594

595 **5. Conclusions**

596 This paper presents the IRIP method for surface runoff susceptibility mapping and its evaluation by
597 comparison with different datasets. The method makes it possible to produce three maps
598 representing different surface runoff mechanisms: generation, transfer, and accumulation. The
599 maps' evaluation shows a significant correspondence between the IRIP map of accumulation and the
600 surface runoff regulatory zoning and between the IRIP map of transfer and the soil erosion zoning.
601 The comparison with data of impacts on the transportation network show promising probabilities of
602 detection which confirm the relevance of the susceptibility maps. For an operational need of network
603 monitoring, the structural vulnerability must be characterized to better discriminate the false alarms.

604 The IRIP method has shown promising results during the comparison tests, but can it be used as a
605 tool for risk management? The IRIP method aims to be simple to implement and requires few input
606 data that are widely available. Neither specific study area size nor calibration is required for a first
607 use. In this sense, the IRIP method can be a useful tool to get a first understanding of the surface
608 runoff mechanisms involved in a catchment and of their spatial distribution. Nonetheless, to go
609 further in the map analysis, field expertise is required. The use of the IRIP maps regarding the usual
610 hazard assessment methods can be complex because of the three types of maps and the
611 susceptibility scale. In the other hand, working with three susceptibility maps of generation, transfer,
612 and accumulation gives the opportunity to adapt risk mitigation techniques depending on the areas.
613 In the areas prone to surface runoff generation, one can avoid soil imperviousness or facilitate
614 infiltration with reservoir basins. In the surface runoff transfer areas, one can avoid bare soils and
615 obstacles susceptible to be swept away. For accumulation areas, one can try to reduce stake
616 vulnerabilities. Finally, this study highlights that a multidisciplinary approach is essential to assess
617 surface runoff hazards. Likewise, a systemic view of the whole catchment is required, along with
618 interactive work with the catchment stakeholders, to improve surface runoff risk management and
619 to sustainably develop territories.

620

621

622

623 **Acknowledgments**

624 We thank all the project contributors: the agglomeration of Le Havre (CODAH) and the mixed
625 association of the Pointe de Caux Catchment (SMBV) for their active contributions by providing high-
626 quality data sets and by remaining available to discuss and analyze the IRIP maps. We also thank the
627 French National Railway Company (SNCF) for its interest in continuing the development of the IRIP

628 method with the IRIP Rail project that funds the development of the iRIP software, and its
629 implementation for the French railway network. We thank Mark Cheetham, engineer at SNCF, for his
630 proofreading and remarks. Finally, we thank ANRT (Agence Nationale de la Recherche et de la
631 Technologie) for partial funding of this work.

632 **References**

- 633 Abudi, I., Carmi, G., Berliner, P., 2012. Rainfall simulator for field runoff studies. *J. Hydrol.* 454, 76–81.
- 634 Akgun, A., Türk, N., 2010. Landslide susceptibility mapping for Ayvalik (Western Turkey) and its
635 vicinity by multicriteria decision analysis. *Environ. Earth Sci.* 61, 595–611.
- 636 Arnaud, P., Dehotin, J., 2011. Surface runoff hazard estimation methods - Comparison of the SHYREG
637 and the IRIP methods. IRSTEA Aix-en-Provence et IRSTEA Lyon.
- 638 Auzet, A.V., Boiffin, J., Papy, F., Ludwig, B., Maucorps, J., 1993. Rill erosion as a function of the
639 characteristics of cultivated catchments in the north of France. *Catena* 20, 41–62.
640 doi:10.1016/0341-8162(93)90028-N
- 641 Bardossy, A., Schmidt, F., 2002. GIS approach to scale issues of perimeter-based shape indices for
642 drainage basins. *Hydrol. Sci. J.-J. Sci. Hydrol.* 47, 931–942. doi:10.1080/02626660209493001
- 643 Bendjoudi, H., Hubert, P., 2002. The Gravelius compactness coefficient: critical analysis of a shape
644 index for drainage basins. *Hydrol. Sci. J.* 47, 921–930. doi:10.1080/02626660209493000
- 645 Beven, K.J., Kirkby, M.J., 1979. A physically based, variable contributing area model of basin
646 hydrology / Un modèle à base physique de zone d'appel variable de l'hydrologie du bassin
647 versant. *Hydrol. Sci. J.* 24, 43–69. doi:10.1080/02626667909491834
- 648 Buckle, P., Mars, G., Smale, S., 2000. New approaches to assessing vulnerability and resilience. *Aust.*
649 *J. Emerg. Manag.* 15, 8.
- 650 Carpenter, T.M., Sperflage, J.A., Georgakakos, K.P., Sweeney, T., Fread, D.L., 1999. National
651 threshold runoff estimation utilizing GIS in support of operational flash flood warning
652 systems. *J. Hydrol.* 224, 21–44. doi:10.1016/S0022-1694(99)00115-8
- 653 Cerdà, A., 2007. Soil water erosion on road embankments in eastern Spain. *Sci. Total Environ.* 378,
654 151–155. doi:10.1016/j.scitotenv.2007.01.041
- 655 Cerdà, A., Doerr, S.H., 2008. The effect of ash and needle cover on surface runoff and erosion in the
656 immediate post-fire period. *Catena* 74, 256–263. doi:10.1016/j.catena.2008.03.010
- 657 Cerdan, O., Souchere, V., Lecomte, V., Couturier, A., Le Bissonnais, Y., 2002. Incorporating soil surface
658 crusting processes in an expert-based runoff model: Sealing and Transfer by Runoff and
659 Erosion related to Agricultural Management. *Catena* 46, 189–205. doi:10.1016/S0341-
660 8162(01)00166-7
- 661 Chazelle, B., Lambert, L., Capoccioni, C.P., 2014. Railway vulnerability in case of extremes floods.
662 Knowledge and risk management. *Houille Blanche* 48–54. doi:10.1051/lhb/2014016
- 663 Christensen, F.M., Andersen, O., Duijm, N.J., Harremoës, P., 2003. Risk terminology—a platform for
664 common understanding and better communication. *J. Hazard. Mater.* 103, 181–203.
665 doi:10.1016/S0304-3894(03)00039-6
- 666 Cros-Cayot, S., 1996. Distribution spatiale des transferts de surface à l'échelle du versant. Contexte
667 armoricain. Ecole Nationale Supérieure Agronomique de Rennes.
- 668 Dabney, S.M., Yoder, D.C., Vieira, D.A.N., Bingner, R.L., 2011. Enhancing RUSLE to include runoff-
669 driven phenomena. *Hydrol. Process.* 25, 1373–1390. doi:10.1002/hyp.7897
- 670 Daroussin, J., King, D., 1997. A pedotransfer rules database to interpret the soil geographical
671 database of Europe for environmental purposes. Presented at the the workshop on the use
672 of pedotransfer in soil hydrology research in Europe, Orléans, FRA, pp. 25–40.
- 673 Defrance, D., 2014. Adaptation and evaluation of a flash flood warning system in ungauged
674 mountainous catchments (Earth Sciences). Université Pierre et Marie Curie - Paris VI.
- 675 Dehotin, J., Breil, P., 2011a. Technical report of the IRIP project: mapping the flooding by runoff
676 (Technical report). IRSTEA Hydrology-Hydraulic Research Unit.
- 677 Dehotin, J., Breil, P., 2011b. IRIP project: Research bibliographic report on surface runoff mapping
678 (Literature review). IRSTEA Hydrology-Hydraulic Research Unit.
- 679 Dehotin, J., Breil, P., Braud, I., de Lavenne, A., Lagouy, M., Sarrazin, B., 2015a. Detecting surface
680 runoff location in a small catchment using distributed and simple observation method. *J.*
681 *Hydrol.* 525, 113–129. doi:10.1016/j.jhydrol.2015.02.051

- 682 Dehotin, J., Chazelle, B., Laverne, G., Hasnaoui, A., Lambert, L., Breil, P., Braud, I., 2015b. Applying
683 runoff mapping method IRIP for flooding risk analysis on railway infrastructure. *Houille*
684 *Blanche* 56–64. doi:10.1051/lhb/20150069
- 685 Delahaye, D., Guermond, Y., Langlois, P., 2002. Spatial interaction in the run-off process. *Cybergeo*
686 *Eur. J. Geogr.* doi:10.4000/cybergeo.3795
- 687 Departmental Directorate of Seine-Maritime, 2013a. Flood Risk Prevention Plan - Presentation
688 report.
- 689 Departmental Directorate of Seine-Maritime, 2013b. Flood Risk Prevention Plan of the Lezarde
690 Catchment - Application rules.
- 691 DeRoo, A.P.J., Wesseling, C.G., Ritsema, C.J., 1996. LISEM: A single-event physically based
692 hydrological and soil erosion model for drainage basins .1. Theory, input and output. *Hydrol.*
693 *Process.* 10, 1107–1117. doi:10.1002/(SICI)1099-1085(199608)10:8<1107::AID-
694 HYP415>3.0.CO;2-4
- 695 Douvinet, J., 2008. Les bassins versants sensibles aux « crues rapides » dans le Bassin Parisien –
696 Analyse de la structure et de la dynamique de systèmes spatiaux complexes. Université de
697 Caen/Basse-Normandie.
- 698 Douvinet, J., Delahaye, D., Langlois, P., 2008. Modélisation de la dynamique potentielle d’un bassin
699 versant et mesure de son efficacité structurelle. *Cybergeo Eur. J. Geogr.*
700 doi:10.4000/cybergeo.16103
- 701 Douvinet, J., Wiel, M.J.V.D., Delahaye, D., Cossart, E., 2014. A flash flood hazard assessment in dry
702 valleys (northern France) by cellular automata modelling. *Nat. Hazards* 75, 2905–2929.
703 doi:10.1007/s11069-014-1470-3
- 704 Dupuis, J., 1969. La carte pédologique de la France au millionième. *Rev. Géographie Alp.* 219–219.
- 705 Faulkner, H., Boardman, J., Ruiz, J.-L., 2010. A simple validated GIS expert system to map relative soil
706 vulnerability and patterns of erosion during the muddy floods of 2000–2001 on the South
707 Downs, Sussex, UK. *Land Degrad. Dev.* 21, 310–321. doi:10.1002/ldr.1005
- 708 Galevski, M., 1955. La corrélation entre les pluies torrentielles et l’intensité de l’érosion (Field
709 observation report).
- 710 Gouvazé, J., SMBV, 2013. Floods of 13 & 14 October 2013: feedback on this unusual weather event.
- 711 Gravelius, H., 1914. *Grundriss der gesamten Gewässerkunde: in vier Bänden. 1. Flusskunde,*
712 *Compendium of Hydrology, vol. 1: Rivers.* Göschen, Berlin, Germany.
- 713 Guillobez, S., Lompo, F., De Noni, G., 2000. Le suivi de l’érosion pluviale et hydrique au Burkina Faso.
714 Utilisation d’un modèle cartographique. *Sci. Chang. Planétaires Sécher.* 11, 163–9.
- 715 Hagen-Zanker, A., 2009. An improved Fuzzy Kappa statistic that accounts for spatial autocorrelation.
716 *Int. J. Geogr. Inf. Sci.* 23, 61–73. doi:10.1080/13658810802570317
- 717 Hargrove, W.W., Hoffman, F.M., Hessburg, P.F., 2006. Mapcurves: a quantitative method for
718 comparing categorical maps. *J. Geogr. Syst.* 8, 187–208. doi:10.1007/s10109-006-0025-x
- 719 Hauchard, E., 2002. Risk Prevention Plan for floods and surface runoff. *Methodol. Defin. Surf. Runoff*
720 *Hazard Hydrogeomorphological Approach Dep. Equip. Dir.* 76.
- 721 Hauchard, E., Delahaye, D., Freiré-Díaz, S., 2002. Fractal organization of the soil occupation:
722 consequences on the runoff and gully erosion in arable cropping areas. *Géomorphologie*
723 *Relief Process. Environ.* 8, 181–196.
- 724 Hauchard, E., Laignel, B., 2008. Morphotectonic evolution of the north-western margin of the Paris
725 Basin. *Z. Für Geomorphol.* 52, 463–488. doi:10.1127/0372-8854/2008/0052-0463
- 726 Hewlett, J.D., 1982. *Principles of forest hydrology.* University of Georgia Press.
- 727 Hewlett, J.D., Hibbert, A.R., 1967. Factors affecting the response of small watersheds to precipitation
728 in humid areas. *For. Hydrol.* 275–290.
- 729 Hogan, R.J., Mason, I.B., 2012. Deterministic forecasts of binary events. *Forecast Verification Pract.*
730 *Guide Atmospheric Sci. Second Ed.* 31–59. doi:10.1002/9781119960003.ch3
- 731 Holzmann, H., Sereinig, N., 1997. In situ measurements of hillslope runoff components with different
732 types of forest vegetation. *IAHS PRESS WALLINGFORD ENGL* 317–324.

- 733 Horton, R.E., 1933. The role of infiltration in the hydrologic cycle. *Trans. Am. Geophys. Union* 14,
734 446–460. doi:10.1029/TR014i001p00446
- 735 Horton, R.E., 1932. Drainage-basin characteristics. *Trans. Am. Geophys. Union* 13, 350.
736 doi:10.1029/TR013i001p00350
- 737 Hudson, N., 1993. Field measurement of soil erosion and runoff. Food & Agriculture Org.
- 738 IPCC, 2003. IPCC Third Assessment Report - Climate Change 2001: 2.3.2.1 Palaeoclimate proxy
739 indicators.
- 740 Jamagne, M., Hardy, R., King, D., Bornand, M., 1995. La base de données géographique des sols de
741 France. *Etude Gest. Sols* 2, 153–172.
- 742 Javelle, P., Demargne, J., Defrance, D., Pansu, J., Arnaud, P., 2014. Evaluating flash-flood warnings at
743 ungauged locations using post-event surveys: a case study with the AIGA warning system.
744 *Hydrol. Sci. J.* 59, 1390–1402. doi:10.1080/02626667.2014.923970
- 745 Lafren, J., Lane, L., Foster, G., 1991. Wepp - a New Generation of Erosion Prediction Technology. *J.*
746 *Soil Water Conserv.* 46, 34–38.
- 747 Langlois, P., Delahaye, D., 2002. RuiCells, automate cellulaire pour la simulation du ruissellement de
748 surface. *Rev. Int. Géomat.* 12, 461–487.
- 749 Laverne, G., 2013. Application and validation of a runoff areas mapping tool in the railway context:
750 identification of sites subject to flooding by runoff (Master thesis). IRSTEA Hydrology-
751 Hydraulic Research Unit.
- 752 Le Bissonnais, Y., Montier, C., Jamagne, M., Daroussin, J., King, D., 2002. Mapping erosion risk for
753 cultivated soil in France. *Catena* 46, 207–220. doi:10.1016/S0341-8162(01)00167-9
- 754 Le Gouee, P., Delahaye, D., Bermond, M., Marie, M., Douvinet, J., Viel, V., 2010. SCALES: a large-scale
755 assessment model of soil erosion hazard in Basse-Normandie (northern-western France).
756 *Earth Surf. Process. Landf.* 35, 887–901. doi:10.1002/esp.1942
- 757 Legros, J., 2014. Study of datas given by a method of flooding hazard by surface runoff in flow
758 discharge modelling linked with this kind of flooding (Master thesis). IRSTEA Hydrology-
759 Hydraulic Research Unit.
- 760 MacQueen, J., 1967. Some methods for classification and analysis of multivariate observations.
761 Presented at the the fifth Berkeley symposium on mathematical statistics and probability,
762 Oakland, CA, USA., pp. 281–297.
- 763 Moriasi, D.N., Arnold, J.G., Van Liew, M.W., Bingner, R.L., Harmel, R.D., Veith, T.L., 2007. Model
764 evaluation guidelines for systematic quantification of accuracy in watershed simulations.
765 *Trans. Asabe* 50, 885–900. doi:10.13031/2013.23153
- 766 Naulin, J.-P., Payrastre, O., Gaume, E., 2013. Spatially distributed flood forecasting in flash flood
767 prone areas: Application to road network supervision in Southern France. *J. Hydrol.* 486, 88–
768 99. doi:10.1016/j.jhydrol.2013.01.044
- 769 Nearing, M.A., Foster, G.R., Lane, L.J., Finkner, S.C., 1989. Erosion Prediction Project Technology.
- 770 Onda, Y., Komatsu, Y., Tsujimura, M., Fujihara, J., 2001. The role of subsurface runoff through
771 bedrock on storm flow generation. *Hydrol. Process.* 15, 1693–1706. doi:10.1002/hyp.234
- 772 Ortega, K.L., Smith, T.M., Manross, K.L., Kolodziej, A.G., Scharfenberg, K.A., Witt, A., Gourley, J.J.,
773 2009. The severe hazards analysis and verification experiment. *Bull. Am. Meteorol. Soc.* 90,
774 1519–1530.
- 775 Pams-Capoccioni, C., Nivon, D., Amblard, J., De cesare, G., Ghilardi, T., 2015. Risk analysis for railway
776 traffic of overflowing of the drainage system on High Speed Lines. *Houille Blanche* 39–45.
777 doi:10.1051/lhb/20150044
- 778 Piney, S., 2009. Etude bibliographique de trois méthodologies appliquées au risque érosion: synthèse
779 et perspective en vue d’une cartographie départementale du risque de ruissellement.
- 780 Pons, F., Delgado, J.-L., Guero, P., Berthier, E., Kerloc’h, B., Piney, S., Felts, D., 2010. A method for the
781 assessment of the flood risk related to direct runoff and flash floods. *SimHydro 2010 Sophia*
782 *Antipolis*.
- 783 Reuter, H.I., Wendroth, O., Kersebaum, K.C., 2006. Optimisation of relief classification for different
784 levels of generalisation. *Geomorphology* 77, 79–89. doi:10.1016/j.geomorph.2006.01.001

- 785 Robinson, D.A., Phillips, C.P., 2001. Crust development in relation to vegetation and agricultural
786 practice on erosion susceptible, dispersive clay soils from central and southern Italy. *Soil*
787 *Tillage Res.* 60, 1–9. doi:10.1016/S0167-1987(01)00166-0
- 788 Schmocker-Fackel, P., Naef, F., Scherrer, S., 2007. Identifying runoff processes on the plot and
789 catchment scale. *Hydrol. Earth Syst. Sci.* 11, 891–906. doi:10.5194/hess-11-891-2007
- 790 Schumm, S.A., 1956. Evolution of drainage systems and slopes in badlands at Perth Amboy, New
791 Jersey. *Geol. Soc. Am. Bull.* 67, 597–646. doi:10.1130/0016-
792 7606(1956)67[597:EODSAS]2.0.CO;2
- 793 Smith, R.E., Goodrich, D.C., Woolhiser, D.A., Unkrich, C.L., 1995. KINEROS-A kinematic runoff and
794 erosion model. *Comput. Models Watershed Hydrol.* 20, 627–668.
- 795 Stanski, H.R., Wilson, L.J., Burrows, W.R., 1989. Survey of common verification methods in
796 meteorology. World Meteorological Organization Geneva.
- 797 Tetzlaff, D., Soulsby, C., Waldron, S., Malcolm, I.A., Bacon, P.J., Dunn, S.M., Lilly, A., Youngson, A.F.,
798 2007. Conceptualization of runoff processes using a geographical information system and
799 tracers in a nested mesoscale catchment. *Hydrol. Process.* 21, 1289–1307.
800 doi:10.1002/hyp.6309
- 801 Thywissen, K., 2006. Components of risk: a comparative glossary. UNU- EHS.
- 802 UNDHA, 1992. Internationally agreed glossary of basic terms related to disaster management. UN
803 DHA U. N. Dep. Humanit. Aff. Geneva.
- 804 UNDRO, 1979. Natural disasters and vulnerability analysis : report of Expert Group Meeting (No.
805 naturaldisasters00offi). Geneva.
- 806 Versini, P.-A., Gaume, E., Andrieu, H., 2010a. Assessment of the susceptibility of roads to flooding
807 based on geographical information - test in a flash flood prone area (the Gard region,
808 France). *Nat. Hazards Earth Syst. Sci.* 10, 793–803. doi:/10/793/2010/
- 809 Versini, P.-A., Gaume, E., Andrieu, H., 2010b. Application of a distributed hydrological model to the
810 design of a road inundation warning system for flash flood prone areas. *Nat. Hazards Earth*
811 *Syst. Sci.* 10, 805–817. doi:/10/805/2010/
- 812 Wischmeier, W.H., 1959. A Rainfall Erosion Index for a Universal Soil-Loss Equation. *Soil Sci. Soc. Am.*
813 *J.* 23, 246. doi:10.2136/sssaj1959.03615995002300030027x
- 814

Figure captions:

Figure 1: Scheme of the IRIP method to create the three susceptibility maps of surface runoff generation, transfer, and accumulation, with the input data

Figure 2: Description of the Lézarde catchment which is located in the Seine-Maritime County and which ranges from 1 to 138 meters of elevation with a short permanent hydrographic network

Figure 3: Description of the rainfall event of October 13, 2013 that impacted the northern part of the Lézarde catchment

Figure 4: Explanative schemes of the data formatting for the comparison with the impact databases, a) Process to detect pixel persistence and remove isolated pixels, b) presentation of the surfaces taken into account for the computation of the contingency table.

Figure 5: The IRIP map of susceptibility of the Lézarde catchment to surface runoff generation

Figure 6: The IRIP map of susceptibility of the Lézarde catchment to surface runoff transfer

Figure 7: The IRIP map of susceptibility of the Lézarde catchment to surface runoff accumulation

Figure 8: Superimposition of the high susceptibility levels of the IRIP map of accumulation and of the surface runoff regulatory zoning

Figure 9: Superimposition of the high susceptibility levels of the IRIP map of transfer and of the soil erosion regulatory zoning

Figure 10: Superimposition of the high susceptibility levels of the IRIP map of transfer and accumulation after processing and of the road network of the three sub-catchments impacted by the rainfall event, along with the road sections impacted by surface runoff and the hydraulic structure locations

Figure 11: Superimposition of the high susceptibility levels of the IRIP map of transfer and accumulation and of the soil erosion regulatory zoning

Figure 12: Photos from Google Street View illustrating the environment configuration around four impacted road sections in order to explain the reason of the IRIP false alarms

Table 1: List of the 5 indicators per map used to create the 3 IRIP maps of generation, transfer, and accumulation susceptibility, with the criteria of favourability for each indicator

Table 2: The theoretical contingency table to analyze the correlation between the IRIP maps and the comparison data

Table 3: The five verification indicators computed to analyze the correlation between the IRIP maps and the comparison data

Table 4: Result summary of the comparison between the regulatory zonings and the high susceptibility levels of the IRIP maps of transfer and accumulation, using buffer area sizes of 0, 25 and 50 meters

Table 5: Result summary of the comparison between the impact locations on the transportation network and the high susceptibility level locations on the IRIP maps of transfer and accumulation, using buffer area sizes of 25 and 50 meters

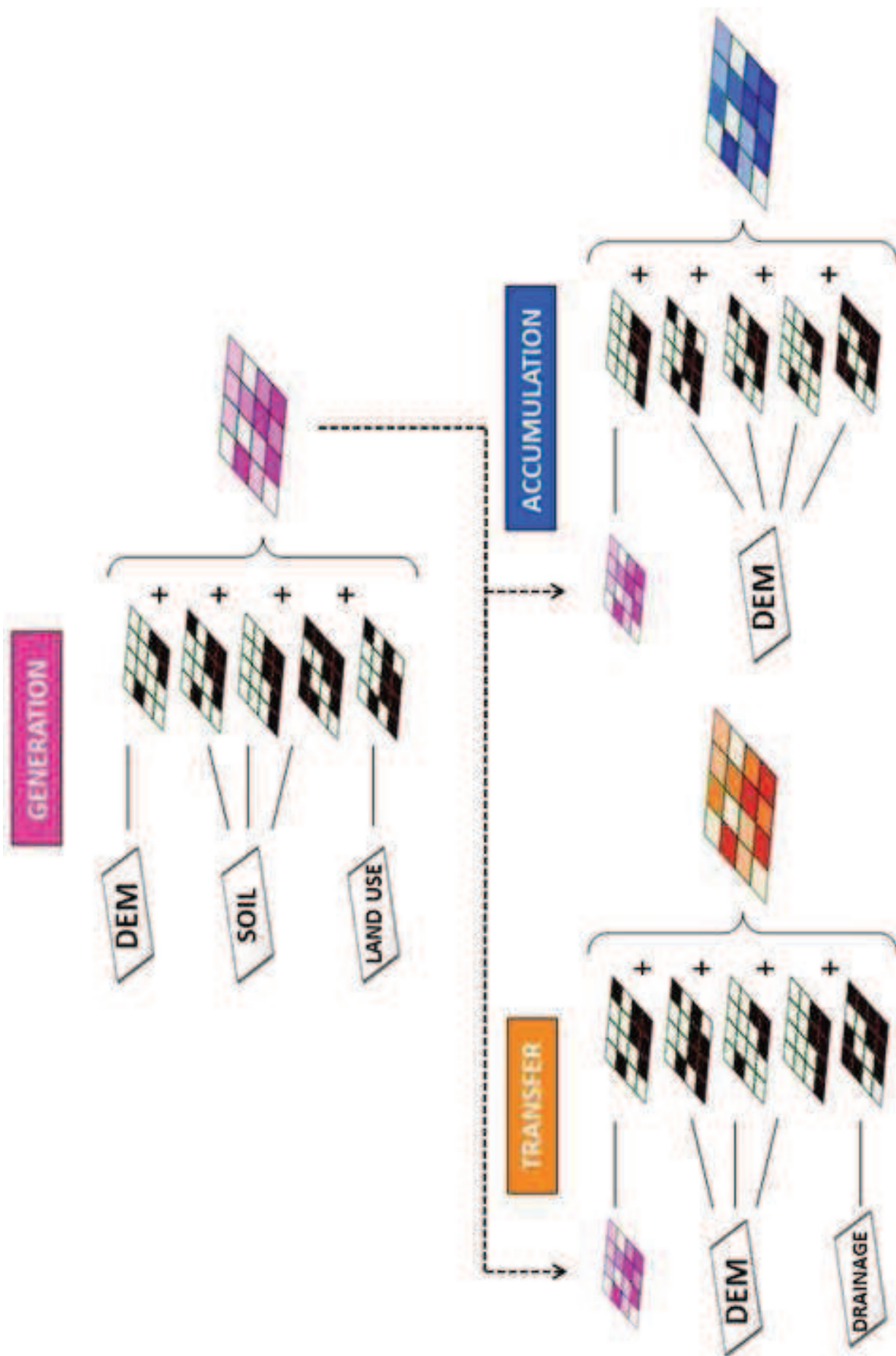


Fig1_the_irip_method_scheme
Click here to download high resolution image

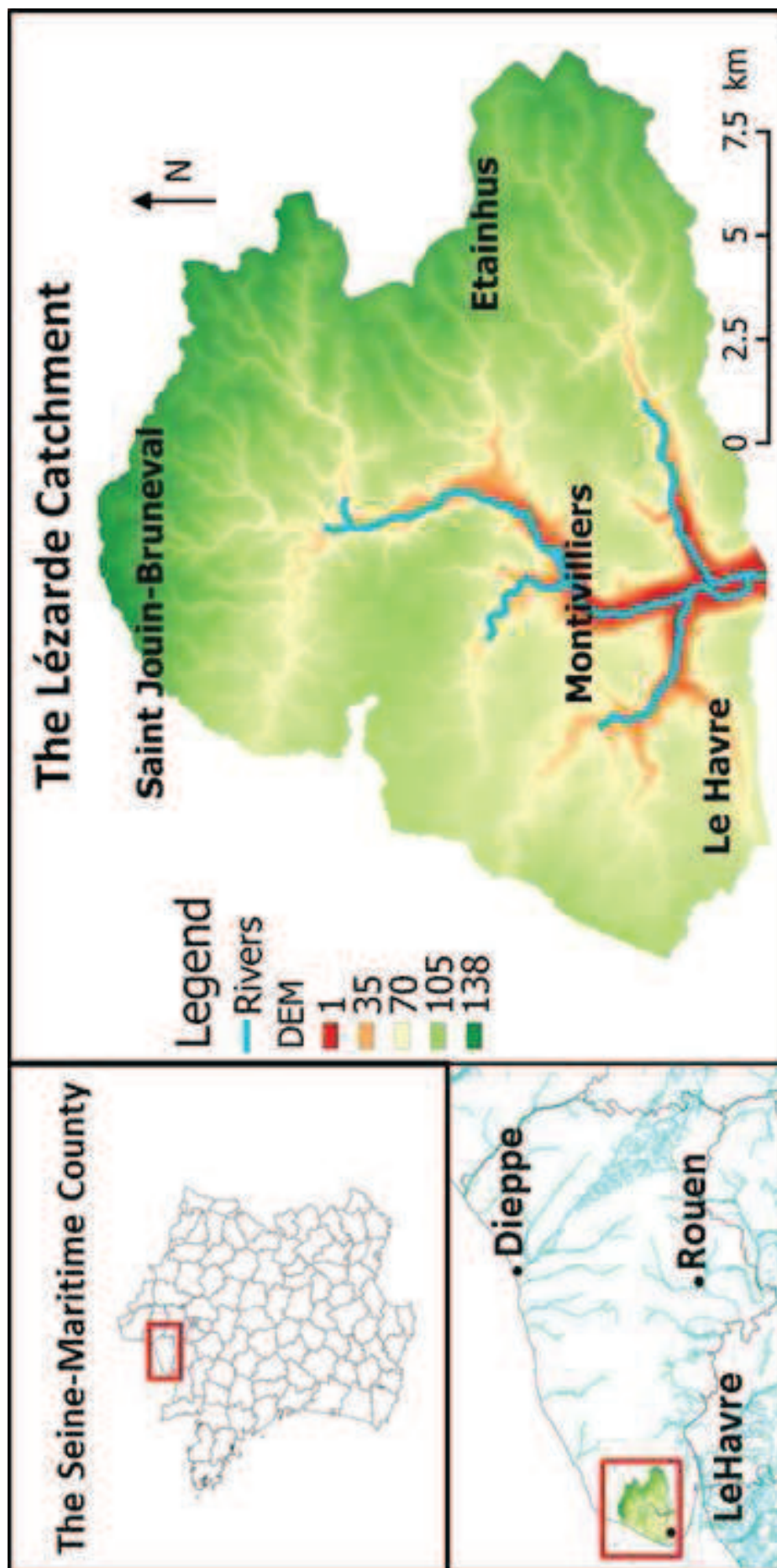


Fig2_the_study_area
Click here to download high resolution image

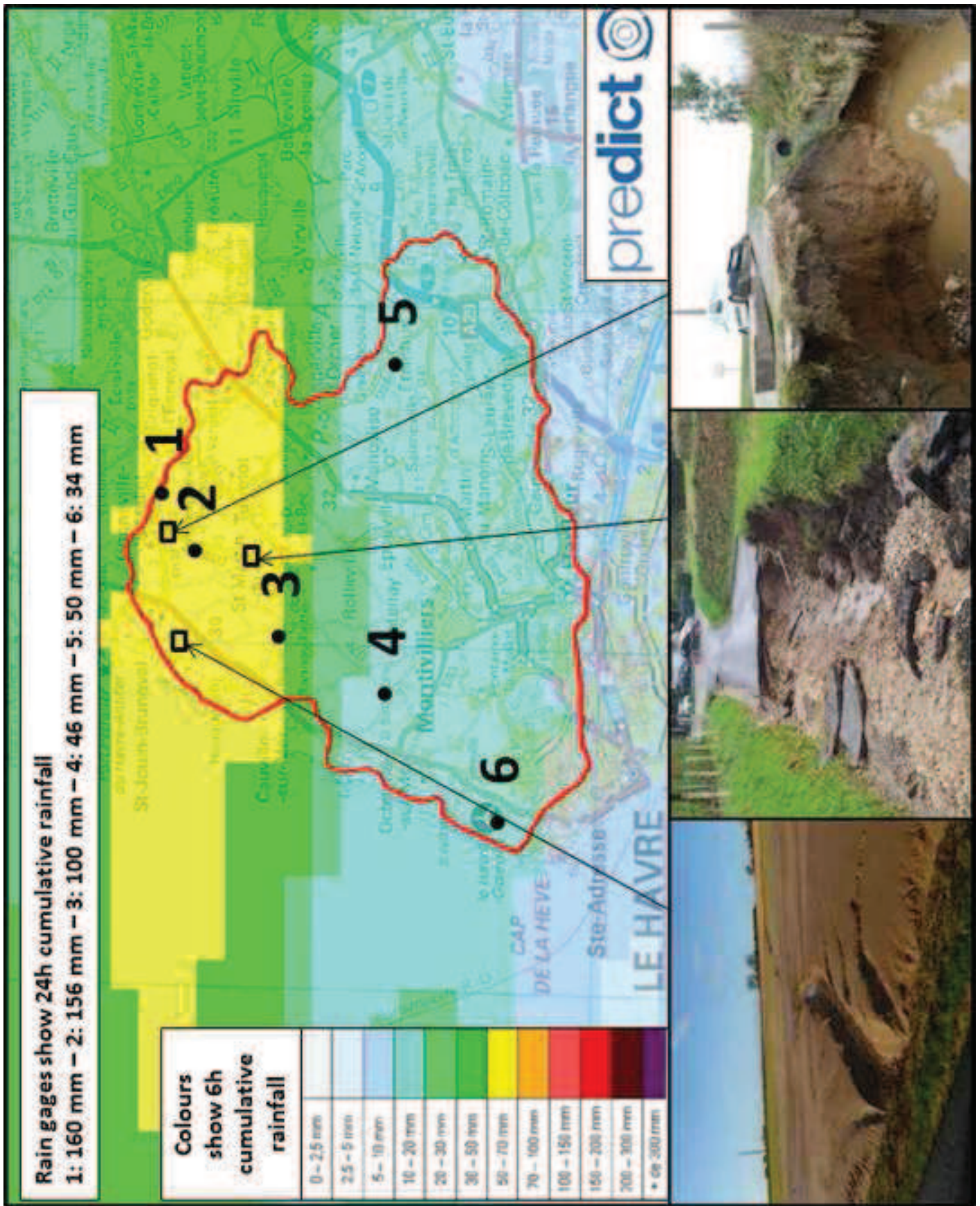


Fig3_Rainfall_13_oct
 Click here to download high resolution image

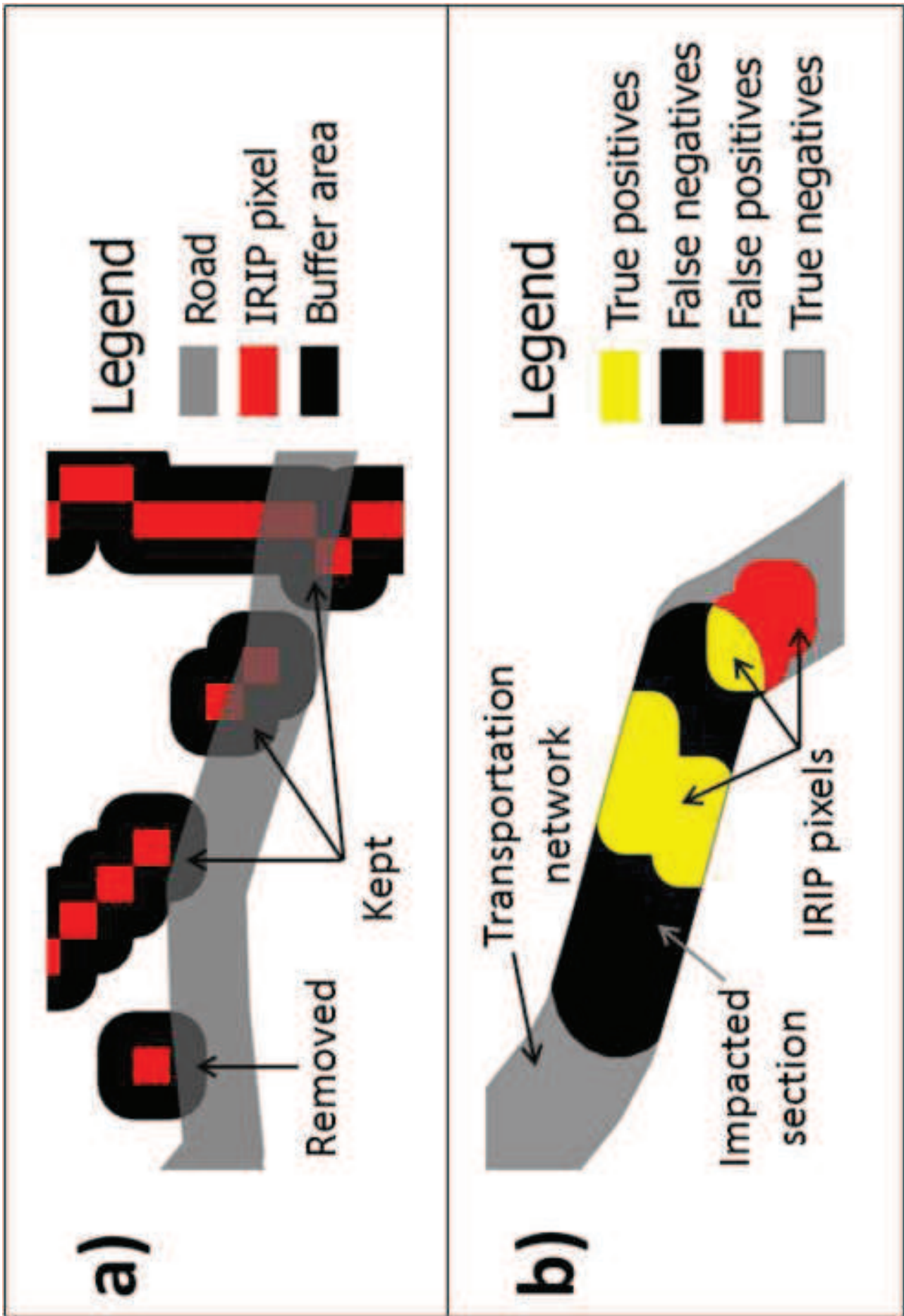


Fig4_detailed_scheme_impact_analysis
[Click here to download high resolution image](#)

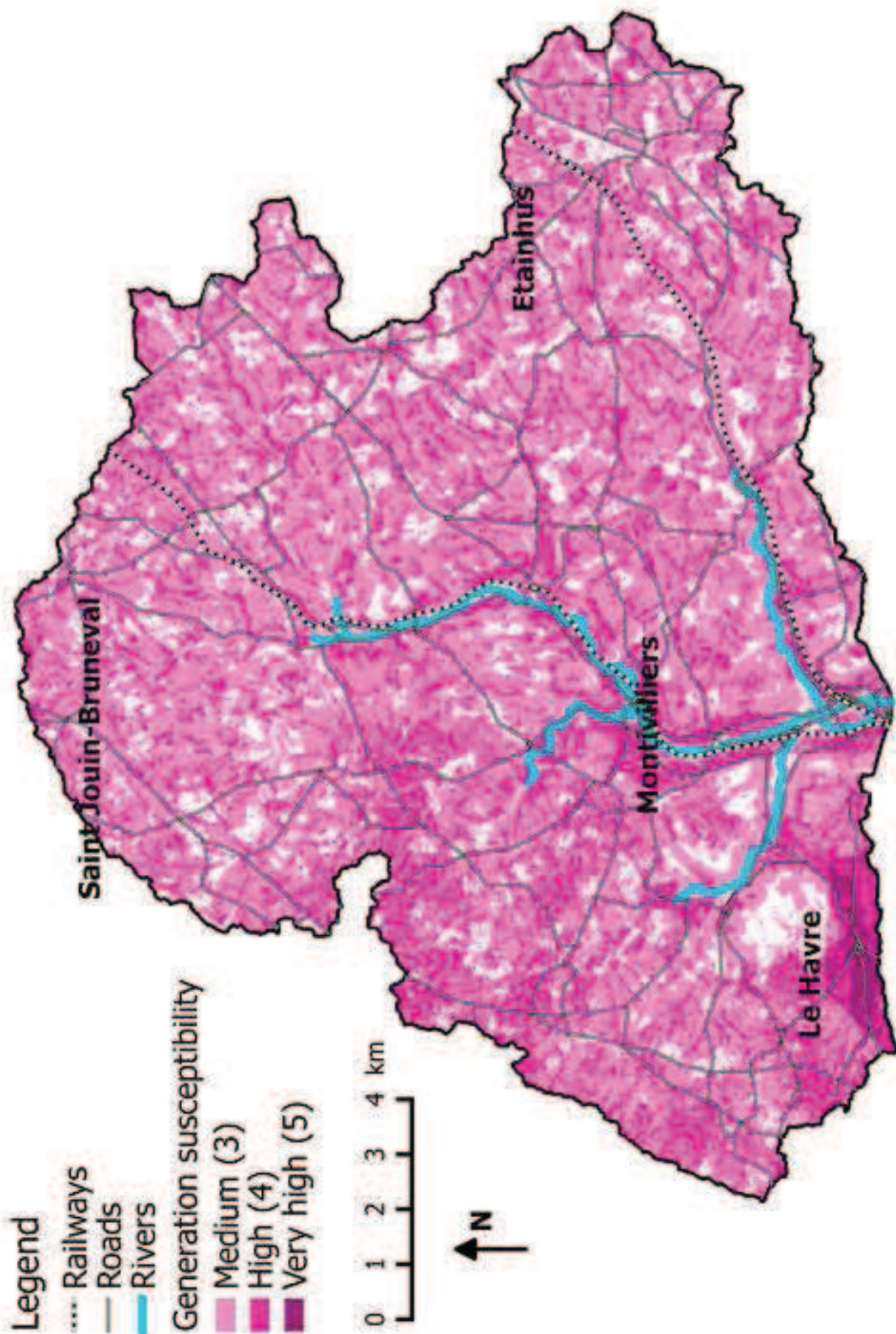


Fig5_IRIP_map_generation
[Click here to download high resolution image](#)

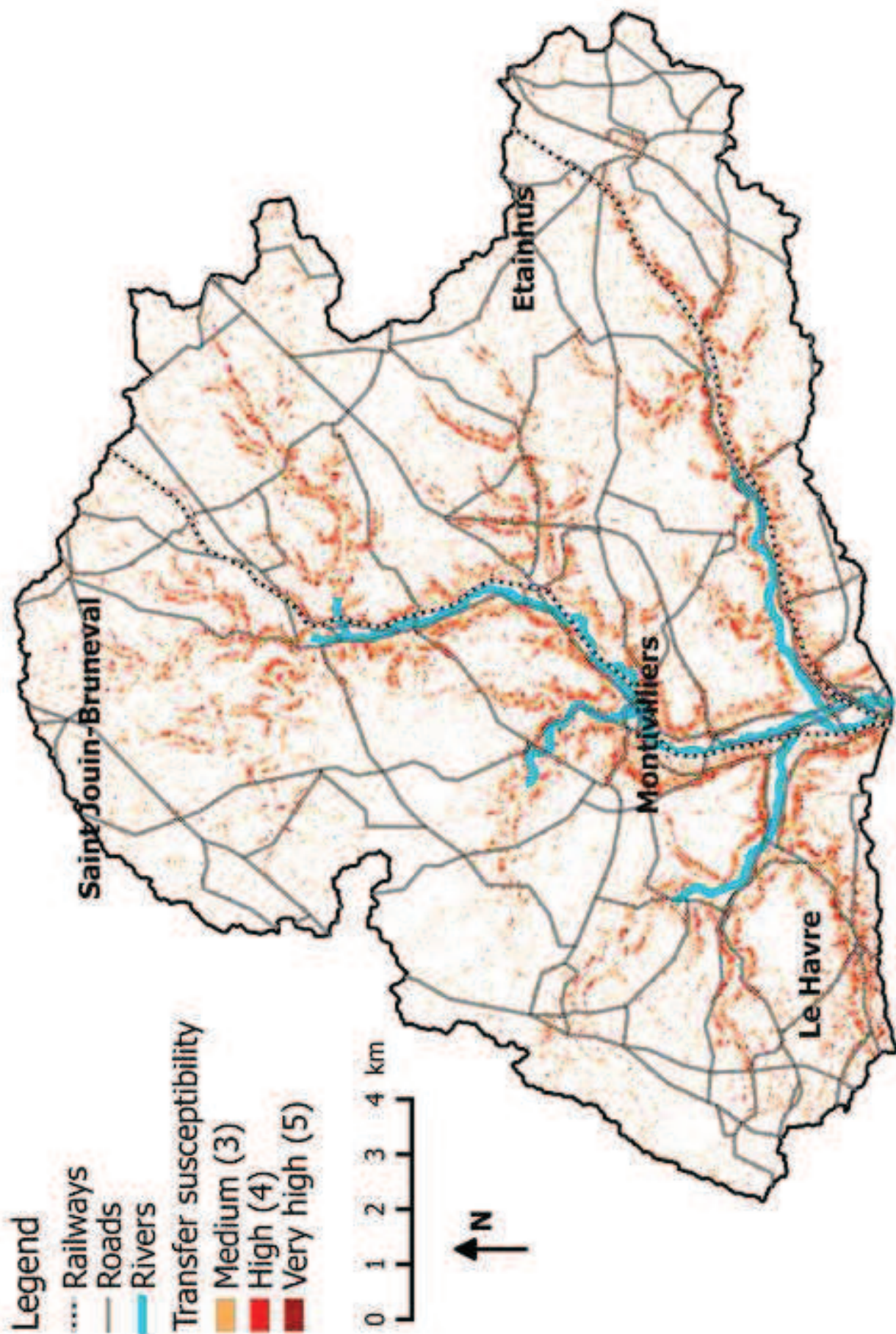


Fig6_IRIP_map_transfer
[Click here to download high resolution image](#)

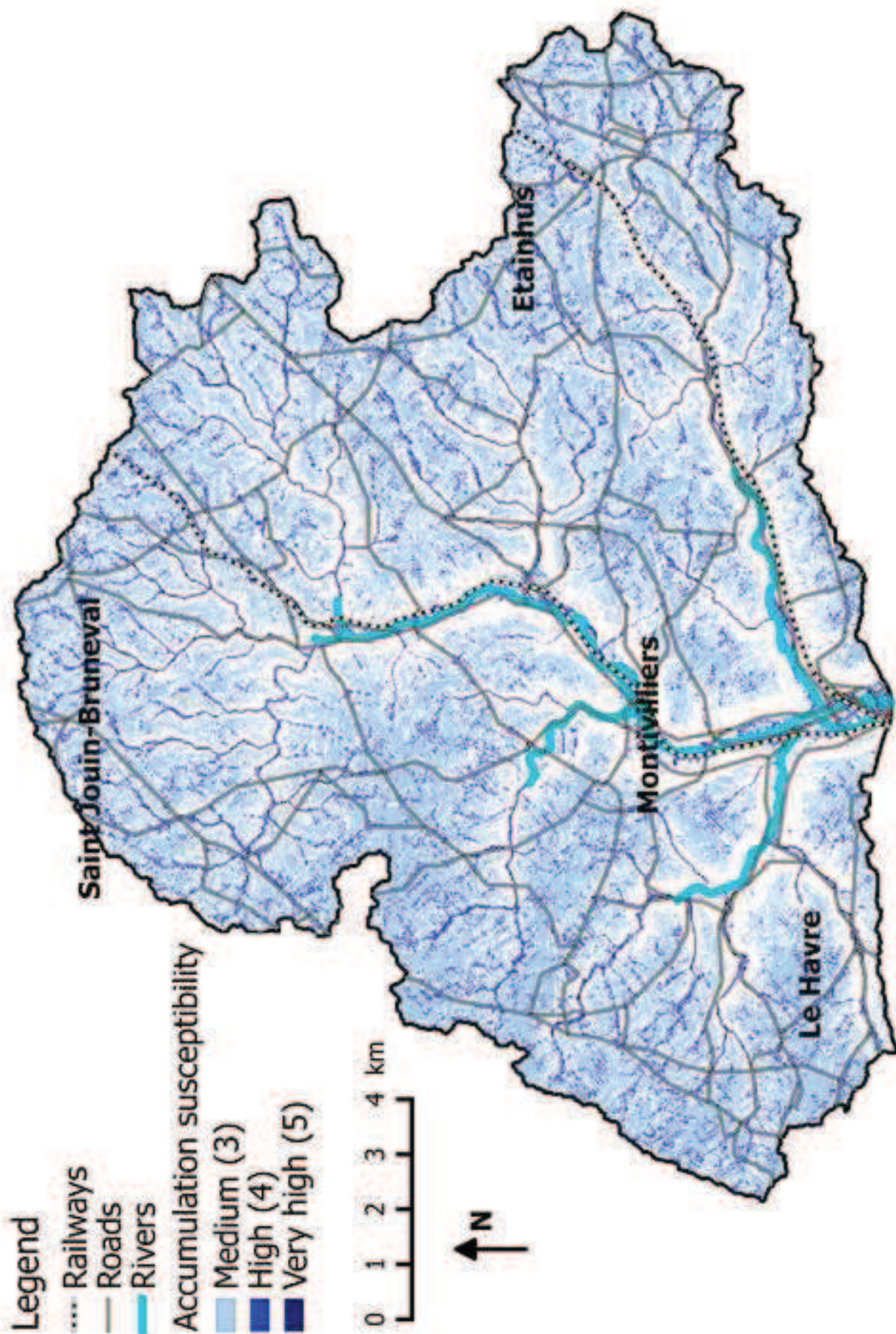


Fig7_IRIP_map_accumulation
Click here to download high resolution image

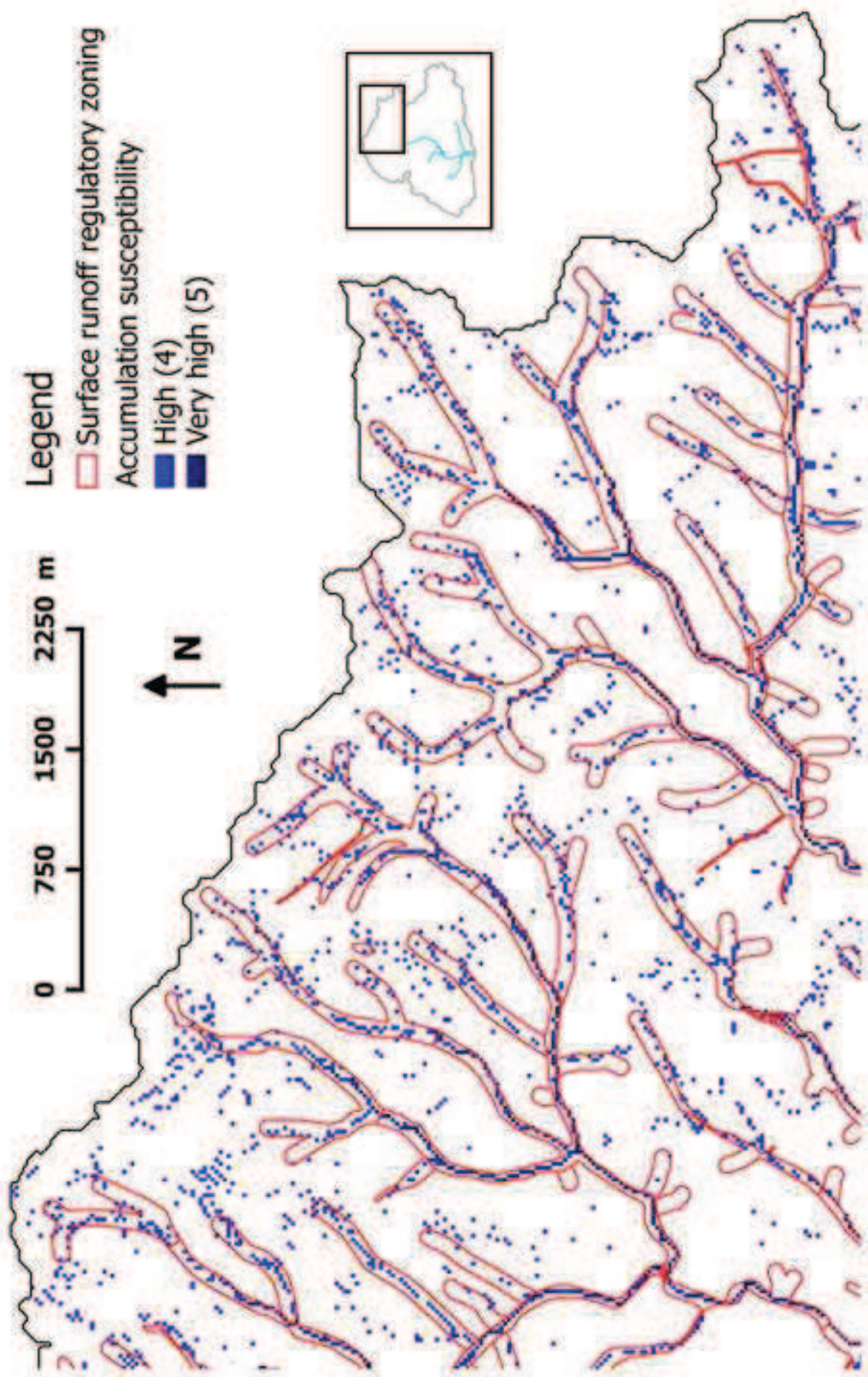


Fig8_comparison_runoff_zoning
[Click here to download high resolution image](#)

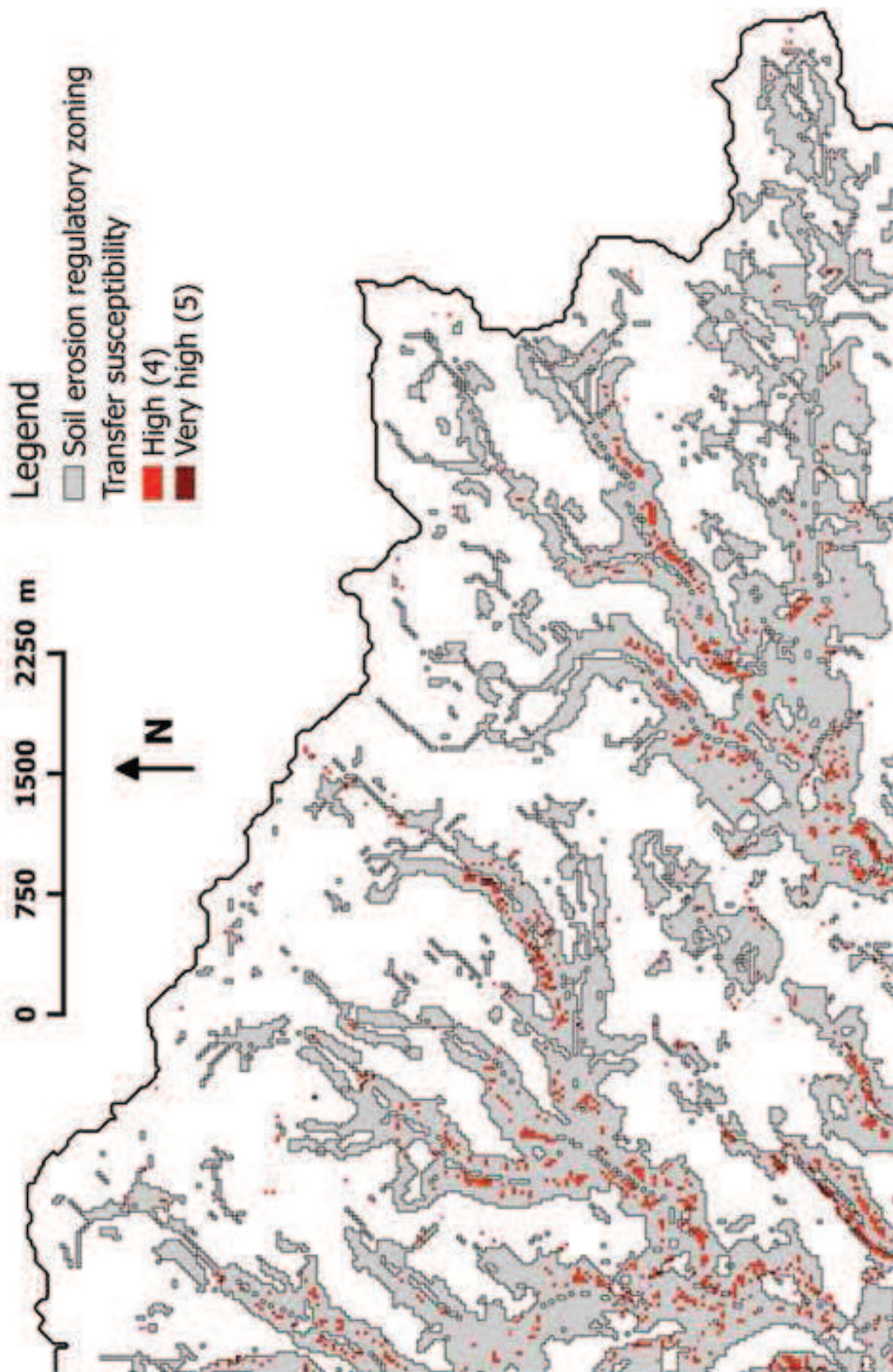


Fig9_comparison_erosion_zoning
[Click here to download high resolution image](#)

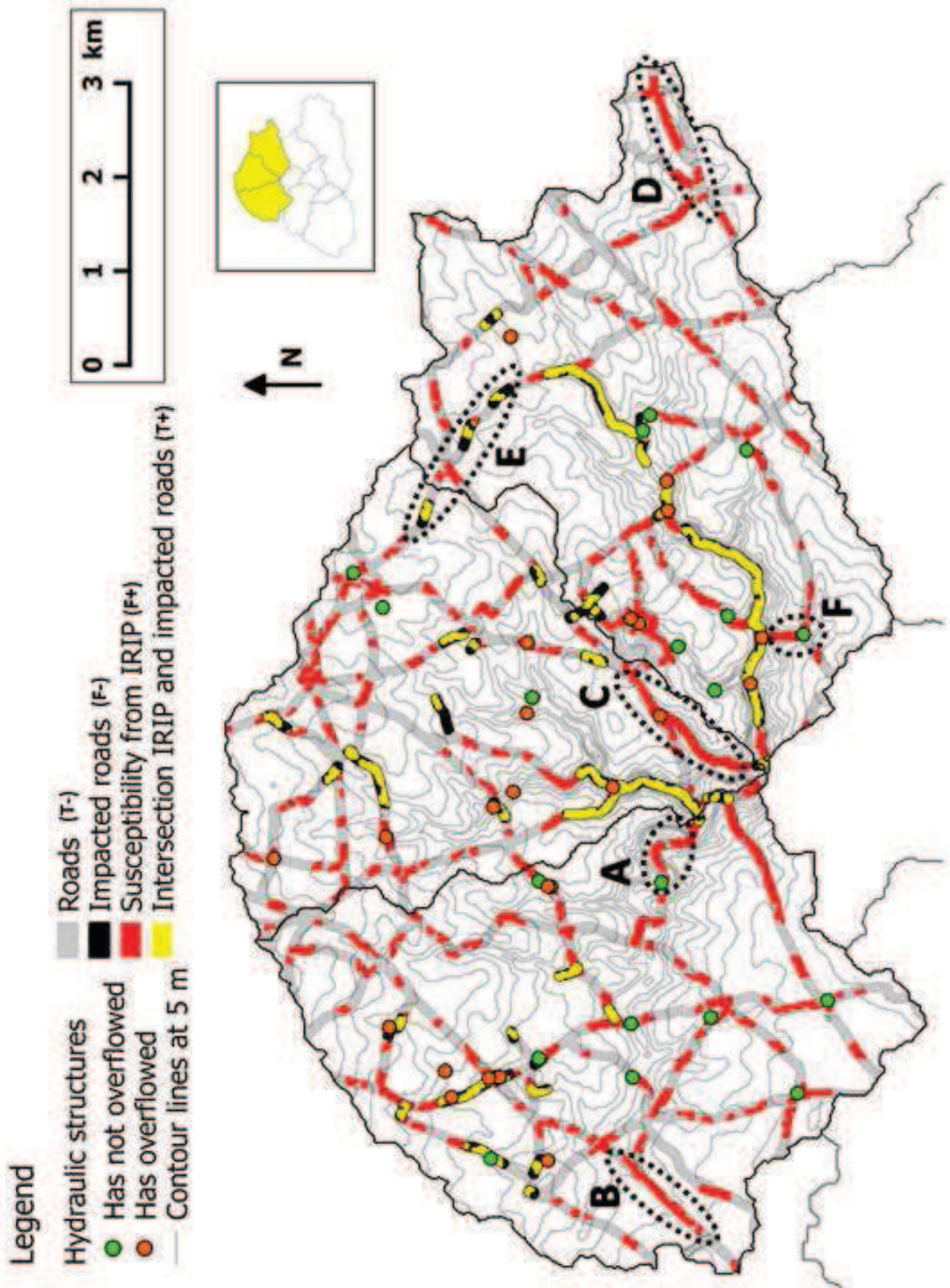


Fig10_road_IRIP_analysis
[Click here to download high resolution image](#)

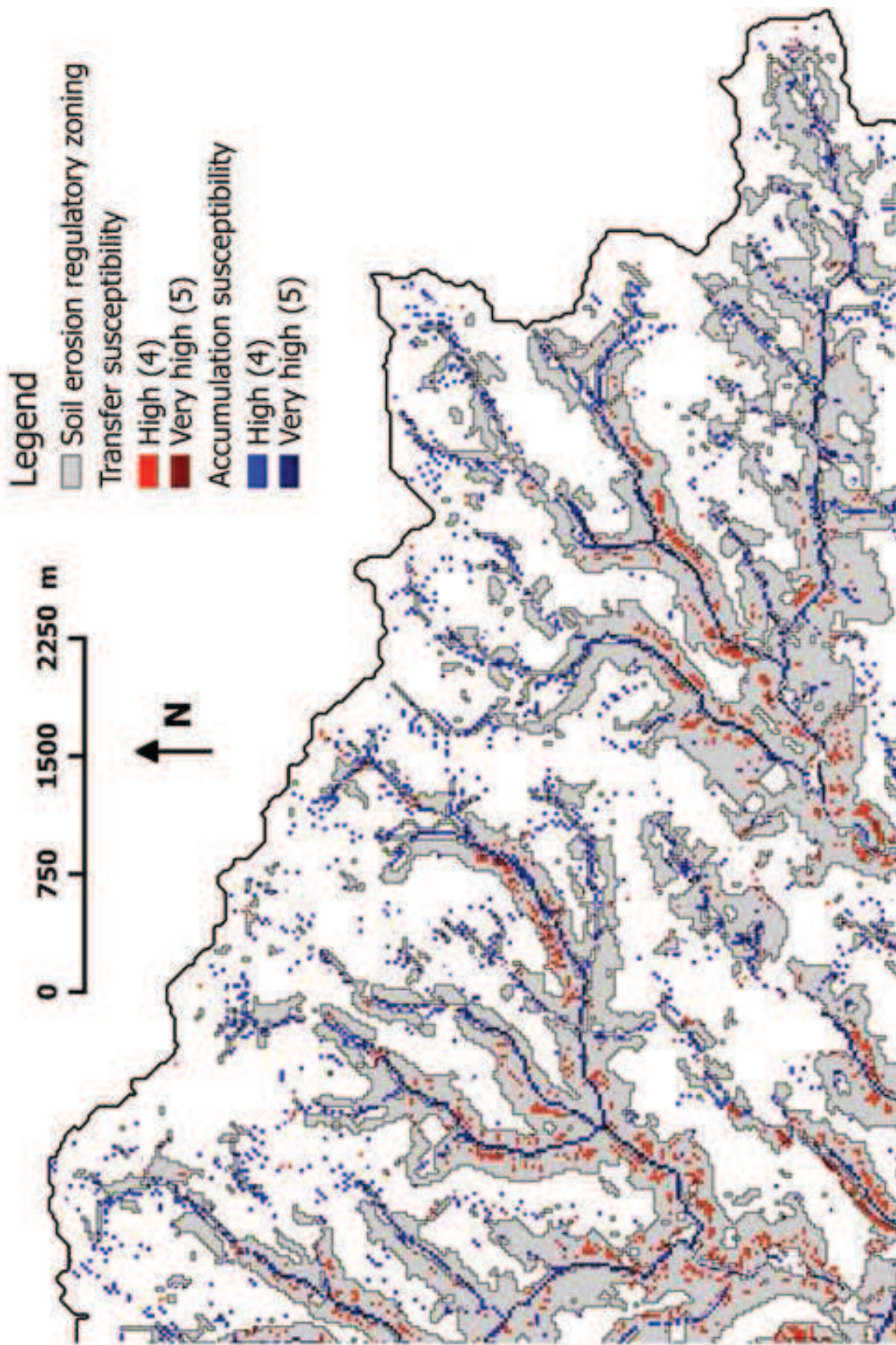


Fig11_comparison_acc_trans_erosion_zoning
[Click here to download high resolution image](#)



Fig12_road_photos_vulnerability
[Click here to download high resolution image](#)

IRIP maps	Indicators	Values
Generation	Soil permeability	0: High permeability
		1: Low permeability
	Soil thickness	0: Thick soil
		1: Thin soil
	Soil erodibility	0: Low erodibility
		1: High erodibility
	Topography	0: Slope < t_1 AND topographic index < t_2
		1: Slope > t_1 OR topographic index > t_2
	Land use	0: Infiltrative surfaces
		1: Impervious surfaces
Transfer	Upstream generation susceptibility	0: Low upstream generation susceptibility
		1: High upstream generation susceptibility
	Slope	0: Slope < t_1
		1: Slope > t_1
	Break of slope	0: Concave break of slope
		1: Convex break of slope
	Catchment compacity	0: Low Horton form factor
		1: High Horton form factor
	Artificial linear axes	0: No linear axes
		1: Presence of linear axes
Accumulation	Upstream generation susceptibility	0: Low upstream generation susceptibility
		1: High upstream generation susceptibility
	Slope	0: Slope > t_1
		1: Slope < t_1
	Break of slope	0: Convex break of slope
		1: Concave break of slope
	Topographic index	0: Topographic index < t_2
		1: Topographic index > t_2
	Flow accumulation	0: Low flow accumulation
		1: High flow accumulation

		Observed event		
		Yes	No	Total
IRIP	Yes	True positives	False positives	Forecast yes
	No	False negatives	True negatives	Forecast no
	Total	Observed yes	Observed no	Total

Verification indicators	Formulas	Interpretation
Accuracy	$\frac{\text{True positives} + \text{True negatives}}{\text{Total}}$	Range: 0 to 1 Perfect score: 1
Bias	$\frac{\text{True positives} + \text{False positives}}{\text{True positives} + \text{False negatives}}$	Range: 0 to ∞ Perfect score: 1 <1 underforecast, >1 overforecast
Success ratio	$\frac{\text{True positives}}{\text{True positives} + \text{False positives}}$	Range: 0 to 1 Perfect score: 1
Probability of detection	$\frac{\text{True positives}}{\text{True positives} + \text{False negatives}}$	Range: 0 to 1 Perfect score: 1
False alarm ratio	$\frac{\text{False positives}}{\text{True positives} + \text{False positives}}$	Range: 0 to 1 Perfect score: 0

IRIP pixels	Verification indicators	Surface runoff zoning / Map of accumulation			Soil erosion zoning / Map of transfer		
		0 m	25 m	50 m	0 m	25 m	50 m
≥4	Accuracy	0.84	0.76	0.68	0.69	0.51	0.39
	Bias	0.41	0.25	0.18	0.12	0.07	0.06
	Success ratio	0.41	0.53	0.59	0.64	0.82	0.91
=5	Accuracy	0.86	0.77	0.68	0.68	0.48	0.36
	Bias	0.06	0.04	0.03	0.01	0.00	0.00
	Success ratio	0.72	0.89	0.92	0.55	0.84	0.92

Verification indicators	Impacts on the transportation network / Maps of transfer and accumulation			
	Roads		Railways	
	25 m	50 m	25 m	50 m
Accuracy	0.68	0.65	0.34	0.30
Bias	3.22	3.10	9.58	7.73
Success ratio	0.23	0.23	0.08	0.12
Probability of detection	0.73	0.72	0.80	0.90
False alarm ratio	0.77	0.77	0.92	0.88